

## Marketing Science

Publication details, including instructions for authors and subscription information:  
<http://pubsonline.informs.org>

### A Theory-Based Explainable Deep Learning Architecture for Music Emotion

Hortense Fong, Vineet Kumar, K. Sudhir

To cite this article:

Hortense Fong, Vineet Kumar, K. Sudhir (2024) A Theory-Based Explainable Deep Learning Architecture for Music Emotion. *Marketing Science*

Published online in Articles in Advance 12 Sep 2024

. <https://doi.org/10.1287/mksc.2022.0323>

Full terms and conditions of use: <https://pubsonline.informs.org/Publications/Librarians-Portal/PubsOnLine-Terms-and-Conditions>

This article may be used only for the purposes of research, teaching, and/or private study. Commercial use or systematic downloading (by robots or other automatic processes) is prohibited without explicit Publisher approval, unless otherwise noted. For more information, contact permissions@informs.org.

The Publisher does not warrant or guarantee the article's accuracy, completeness, merchantability, fitness for a particular purpose, or non-infringement. Descriptions of, or references to, products or publications, or inclusion of an advertisement in this article, neither constitutes nor implies a guarantee, endorsement, or support of claims made of that product, publication, or service.

Copyright © 2024, INFORMS

Please scroll down for article—it is on subsequent pages



With 12,500 members from nearly 90 countries, INFORMS is the largest international association of operations research (O.R.) and analytics professionals and students. INFORMS provides unique networking and learning opportunities for individual professionals, and organizations of all types and sizes, to better understand and use O.R. and analytics tools and methods to transform strategic visions and achieve better outcomes.

For more information on INFORMS, its publications, membership, or meetings visit <http://www.informs.org>

# A Theory-Based Explainable Deep Learning Architecture for Music Emotion

Hortense Fong,<sup>a,\*</sup> Vineet Kumar,<sup>b</sup> K. Sudhir<sup>b</sup>

<sup>a</sup>Marketing, Columbia Business School, New York, New York 10027; <sup>b</sup>Yale School of Management, New Haven, Connecticut 06511

\*Corresponding author

Contact: hf2462@gsb.columbia.edu,  <https://orcid.org/0000-0003-0256-7943> (HF); vineet.kumar@yale.edu,  <https://orcid.org/0000-0001-8784-6858> (VK); k.sudhir@yale.edu,  <https://orcid.org/0000-0001-9398-8887> (KS)

---

Received: September 2, 2022

Revised: October 2, 2023; March 4, 2024

Accepted: May 6, 2024

Published Online in Articles in Advance:  
September 12, 2024

<https://doi.org/10.1287/mksc.2022.0323>

Copyright: © 2024 INFORMS

**Abstract.** This paper develops a theory-based, explainable deep learning convolutional neural network (CNN) classifier to predict the time-varying emotional response to music. We design novel CNN filters that leverage the frequency harmonics structure from acoustic physics known to impact the perception of musical features. Our theory-based model is more parsimonious, but it provides comparable predictive performance with atheoretical deep learning models while performing better than models using handcrafted features. Our model can be complemented with handcrafted features, but the performance improvement is marginal. Importantly, the harmonics-based structure placed on the CNN filters provides better explainability for how the model predicts emotional response (valence and arousal) because emotion is closely related to consonance—a perceptual feature defined by the alignment of harmonics. Finally, we illustrate the utility of our model with an application involving digital advertising. Motivated by YouTube’s midroll ads, we conduct a laboratory experiment in which we exogenously insert ads at different times within videos. We find that ads placed in emotionally similar contexts increase ad engagement (lower skip rates and higher brand recall rates). Ad insertion based on emotional similarity metrics predicted by our theory-based, explainable model produces comparable or better engagement relative to atheoretical models.

---

History: Tat Chan served as the senior editor.

Supplemental Material: The online appendix and data files are available at <https://doi.org/10.1287/mksc.2022.0323>.

---

**Keywords:** audio data • deep learning • explainable and interpretable AI • emotion • digital advertising • music theory

---

## 1. Introduction

Music is widely regarded as among the most effective and efficient of channels to influence emotion; it is often called the *language of emotion* (Corrigall and Schellenberg 2013). As emotions play a central role in many elements of marketing and consumer behavior, marketers routinely use music to evoke emotion along the customer journey, from need recognition to purchase, in advertising, content marketing, and stores (Gorn 1982, Krishna 2012). In particular, music is almost universally used in advertising, and advertisers spend considerable effort crafting it to elicit desired emotions and consequent marketing outcomes.<sup>1</sup> As such, a tool that maps music (or an ad with music) to its evoked emotion can be valuable to marketers. For example, marketers can use such a method to automate emotion-based contextual matching of ads and content at scale to increase ad engagement. On music and video platforms, it can be valuable in automating creation of mood-based playlists and

“next song” recommendations for users from their large collections.<sup>2</sup>

In this paper, we develop a theory-based, explainable deep learning convolutional neural network (CNN) classifier that takes music audio as input and predicts the sequence of emotions it evokes in a listener. We characterize emotion using the well-established valence-arousal framework developed by Russell (1980). Valence measures how positive or negative a listener feels, and higher valence maps to more positive feeling. Arousal measures how energetic a listener feels, and higher arousal maps to greater excitement and energy.<sup>3</sup>

Existing music emotion classifiers can be grouped into two types based on explainability and accuracy, and there is often a trade-off between these. Classifiers using handcrafted features and traditional machine learning methods are typically more explainable but often less accurate, whereas classifiers using data-

driven variables and “atheoretical” deep learning methods are typically less explainable but more accurate. By incorporating theory into the model design, our deep learning model seeks to be both accurate and explainable.

We highlight and explain the two key distinguishing features in the modeling contribution. First and most important, we incorporate music theory based on harmonics in the model. When a musical note is generated, its pitch is characterized by its fundamental frequency (i.e., lowest frequency), and harmonics refer to the whole number multiples of the fundamental frequency. We *design harmonics filters* to capture theoretically known musical features that link to emotion.<sup>4</sup> Such filter construction is challenging because current CNN implementations for music are based on adaptations of models developed for computer vision where *spatial contiguity* is meaningful. In music, however, many important features are dependent on elements that are *noncontiguous*, implying that filters inspired by vision are inadequate and/or inefficient for music. Harmonics, in particular, are by definition based on noncontiguous frequencies and underlie several musical features, like consonance, timbre, and pitch, which have well-established empirical links to emotional response.<sup>5</sup> We, therefore, incorporate structure into the CNN filters based on the role of harmonics, which also helps to create a more parsimonious model without reducing accuracy, relative to benchmark atheoretical models.

Second, our theory-based filters are more explainable relative to atheoretical deep learning models because the filters are designed to characterize features that are well known to impact emotion. To aid explainability, we visualize the link between emotion and the features learned by the theory-based filters. For this, we adapt recent advances in the visualization of deep learning models for computer vision (i.e., gradient-weighted class activation mapping (Grad-CAM)). The focus on explainability allows us to go beyond model prediction, giving researchers and practitioners confidence that the model is learning a feature of the music (i.e., consonance) that can generalize outside of the training data rather than picking up spurious correlations. Explainability helps build trust in the model, which facilitates adoption at scale.<sup>6</sup>

Finally, we illustrate the practical value of our model in an application motivated by YouTube’s midroll video ads. YouTube serves tens of millions of content videos each day; an ad can be placed in a number of different ad breaks within each content video. Given the scale, identifying the optimal ad breaks in the videos for ad insertion requires automation. First, we examine whether matching the ad’s emotion with the emotion of the content at the ad insertion point improves or hurts ad effectiveness. To test this, we conduct a laboratory experiment in which we insert ads at points in videos

that differ in emotional similarity between the ads and content videos. We find that greater emotional similarity helps by decreasing ad skip and increasing brand recall. We then input the audio of the ads and content videos into our model to predict emotion and use the predicted emotion to determine the most emotionally similar ad insertion point for each ad within each content video.<sup>7</sup> The engagement outcomes based on ad insertion using our theory-driven model are comparable with those from ad insertion using atheoretical models, but unlike the atheoretical models, our model is more explainable.

We provide an overview of the elements of our model to help build intuition for the critical challenges in constructing a CNN model for predicting music emotion that is both theory based and explainable. Our methodological approach uses the raw sound wave of a music clip rather than predefined handcrafted features as the starting input. We transform the sound wave into a mel spectrogram, which reflects human hearing and is the input into the CNN. The mel spectrogram visualizes which frequencies are present at any given time.<sup>8</sup> This representation is useful because it allows us to “read” some of the clip’s music features, such as frequency range and note density. Recent research developing and applying CNN for music uses mel spectrograms as input (e.g., Pons et al. 2016, Chowdhury et al. 2019, Rajaram and Manchanda 2024), and we detail the rationale and implementation in Section 3.

CNNs are deep neural networks specially developed for image processing in which objects are contiguous across both *x* and *y* dimensions, which have spatial meaning based on physical reality. Convolution filters play a critical role in determining the performance of CNNs, and the filters designed for image processing take advantage of spatial contiguity to perform effectively. However, spectrograms generated from music are not like regular images. In spectrograms, noncontiguous regions in the frequency space impact many characteristics of music that humans perceive. For example, an octave (e.g., A4 (440 hertz (Hz)) and A5 (880 Hz)) produces a consonant sound, whereas a tritone (e.g., A4 (440 Hz) and D5 (587 Hz)) produces a dissonant sound. Typical square CNN filters, which account for contiguous areas of an image, cannot capture such concepts based on noncontiguous frequencies, thus highlighting the challenge of designing novel filters to incorporate music domain knowledge into deep learning models.<sup>9</sup>

We develop novel noncontiguous filters that specifically incorporate relevant harmonic frequencies into the CNN model. By incorporating the harmonic structure, the filters can more parsimoniously capture many relevant characteristics of music that involve harmonics and their interactions. In particular, they help to identify consonance, which is well known to influence emotional response to music.<sup>10</sup> By leveraging ideas from

music theory to build the model, we set the stage for explainability postestimation.

To aid explainability, we adapt Grad-CAM, a tool that uses a heat map to visualize which areas of an image contribute most to the classification of the image into a specific class (Selvaraju et al. 2017). Consider the problem of classifying images of wolves and huskies. Suppose a CNN trained to distinguish wolves from huskies generates Grad-CAM heat maps that highlight the background of the image as the main predictor because wolves are commonly photographed in snow and huskies are commonly photographed in grass (Ribeiro et al. 2016). If the prediction is driven by the background of snow or grass, a spurious correlation, a new example of a husky playing in snow is more likely to be classified incorrectly as a wolf. With Grad-CAM highlighting the background, we learn that the model did not learn to distinguish between wolves and huskies based on features of the animals themselves but rather, the background of the image, implying that the generalizability of the model is under question. Knowing *why* a model makes various predictions helps assess model generalizability.

In the context of music, relating the top-level outcome or label of interest (e.g., emotion) to a midlevel set of musical features (e.g., consonance, timbre, and rhythm) provides us a clearer understanding of the features responsible for the prediction, making the model more explainable.<sup>11</sup> Although low-level features (e.g., frequency and time) provide some degree of transparency, they do not have a clear explainable link to top-level labels (Fu et al. 2010). Our Grad-CAM visualizations for the theory-based deep learning model highlight areas of high and low consonance in the mel spectrograms consistent with theory linking consonance and emotion. In contrast, heat maps for the model based on atheoretical square filters show a less clear pattern linking musical features to emotion. Broadly, this contrast shows the value of incorporating theory-based structure into CNN filter design for explainability.

Summarizing, our key contributions are as follows. First, we develop a theory-based, explainable deep learning framework that models and predicts time-varying emotional response. Second, our approach of integrating a harmonics-based structure enables model explainability. We show with Grad-CAM that incorporating such structure into the design of the CNN filter allows us to visualize the link between predicted emotion and consonance. Third, the theory-based model produces comparable predictive performance with atheoretical models with much greater parsimony, which in turn, makes the model less complex to train, as well as more generalizable and robust (e.g., Gerg and Monga 2021, Kutz and Brunton 2022). Fourth, we show how additional handcrafted features can be incorporated into our deep learning framework without

impacting explainability. Fifth, we demonstrate the model's practical value with an application that examines the impact of matching the emotion of a video ad with the emotion of the content video.

## 2. Related Literature

Our paper builds upon several distinct streams of literature across fields, as detailed below.

### 2.1. Listener Response to Music

Music induces emotion, as shown by a wide literature using methods ranging from surveys to brain scans (Johnson-Laird and Oatley 2016). Because our focus is on the background music of content and ads, which typically falls under Western tonal music (Nelson et al. 2013, Stoppe 2014), our focus in this paper is on the musical associations between Western tonal music and emotion.<sup>12</sup> In particular, consonance and dissonance play a major role in creating emotion in background music. According to Nelson et al. (2013, p. 89), the manipulation of consonant and dissonant harmonies "is the most immediately effective way a composer can alter the mood of a scene." In Western tonal music, consonance is associated with positive valence and low-arousal emotion, whereas dissonance is associated with negative valence and high-arousal emotion (Gabrielson and Lindström 2010, Thompson and Balkwill 2010). Online Appendix C discusses how timbre and pitch also impact emotional response.

Emotional responses to music have marketing implications, and a substream of the literature focuses on the relationship between music features and marketing outcomes. Bruner (1990) overviews how music elicits different moods, which in turn, impact ad outcomes. Yang et al. (2022) use low-level acoustic features to predict ad audio energy levels and find that energetic commercials are more likely to be watched for longer. Boughanmi and Ansari (2021) use a Bayesian nonparametric approach to predict album sales using multimodal data that include high-level audio features of music in the songs of the albums. Melzner and Raghbir (2023) study how timbre affects judgments of brand personality. More broadly, our research is related to the literature on sensory marketing as music impacts consumers through the auditory sense (Krishna 2012).

### 2.2. Machine Learning with Unstructured Audio Data

Although audio includes both speech and music, our focus in this paper is on music. Traditional machine learning methods, like support vector machine, previously produced good classification performance in many settings by using handcrafted features, such as mel frequency cepstral coefficients. However, the performance of deep learning algorithms has overtaken

almost all other methods in audio applications, similar to vision applications (Hinton et al. 2012). The crucial advantage that deep learning has is that features are automatically learned from data rather than predefined (Choi et al. 2018).

With deep learning, music is typically converted to a spectrogram, which is used as the input to the learning algorithm. A few researchers have attempted to build music-specific deep learning models rather than use CNN models designed for image recognition. For example, to predict ballroom music genre, Pons et al. (2016) suggest using musically motivated CNN filters to capture low-level timbral and temporal elements of music. This translates to using various rectangular convolutional filters—tall and skinny filters for timbral elements and short and wide filters for temporal elements. Using data with labeled emotion and midlevel features (e.g., melodiousness and articulation), Chowdhury et al. (2019) build a deep learning model that includes an interpretable midlevel feature layer to predict emotion. We contribute to the audio machine learning literature by designing and developing novel CNN filters based on harmonics, and we demonstrate how the filters are useful for prediction as well as explanation.

### 2.3. Ad Insertion in Videos

An evolving literature has examined video ads within streaming videos to understand what ad, content video, and user characteristics impact ad performance. For a survey of this literature, see Fraude et al. (2021).<sup>13</sup> The typical outcomes examined in studies of video ads include ad skipping, brand recognition, intrusiveness, aided and unaided brand recall, ad acceptance, click-through rate, and related metrics for ads accompanied by a call to action.

Research focused on ads has explored the impact of ad characteristics, such as length and content, and interactions between ads, such as the number of ads within a break, on outcomes like brand recall (Goodrich et al. 2015). Prior work exploring *both ad and content video characteristics* has studied the impact of ad relevance (e.g., showing a Ford ad in a video about Formula 1 racing) and ad congruence on performance. For ad relevance, Li and Lo (2015) found that for midroll ads, congruence between the ad product and the video content improves consumer receptivity, whereas the opposite is true for postroll ads. For emotional congruence, results have been mixed. Belanche et al. (2017) found in an experiment that high-arousal ads are watched for longer in high-arousal content than in low-arousal content but found no such effect of congruence for low-arousal ads. On the other hand, although not in a video ad insertion context, Puccinelli et al. (2015) found that consumers in a low-arousal state watch high-arousal ads for less time than moderate-arousal ads, supporting congruence. Kapoor et al. (2022) focused on the emotions of

happiness and sadness, and they found in a field experiment that emotional contrast led to greater ad engagement. Overall, the results in the literature are mixed on whether emotional congruence improves ad performance. An important point of contrast for this paper is that relative to past research focusing on the overall emotion in the content video for ad matching, our focus is on the time-varying emotion of the content video to identify the optimal emotion-based ad insertion position within the video.

## 3. Deep Learning Model for Music Emotion

We develop a CNN for emotion classification that incorporates theory relating to the physics of sound waves and the perception of Western tonal music by listeners.

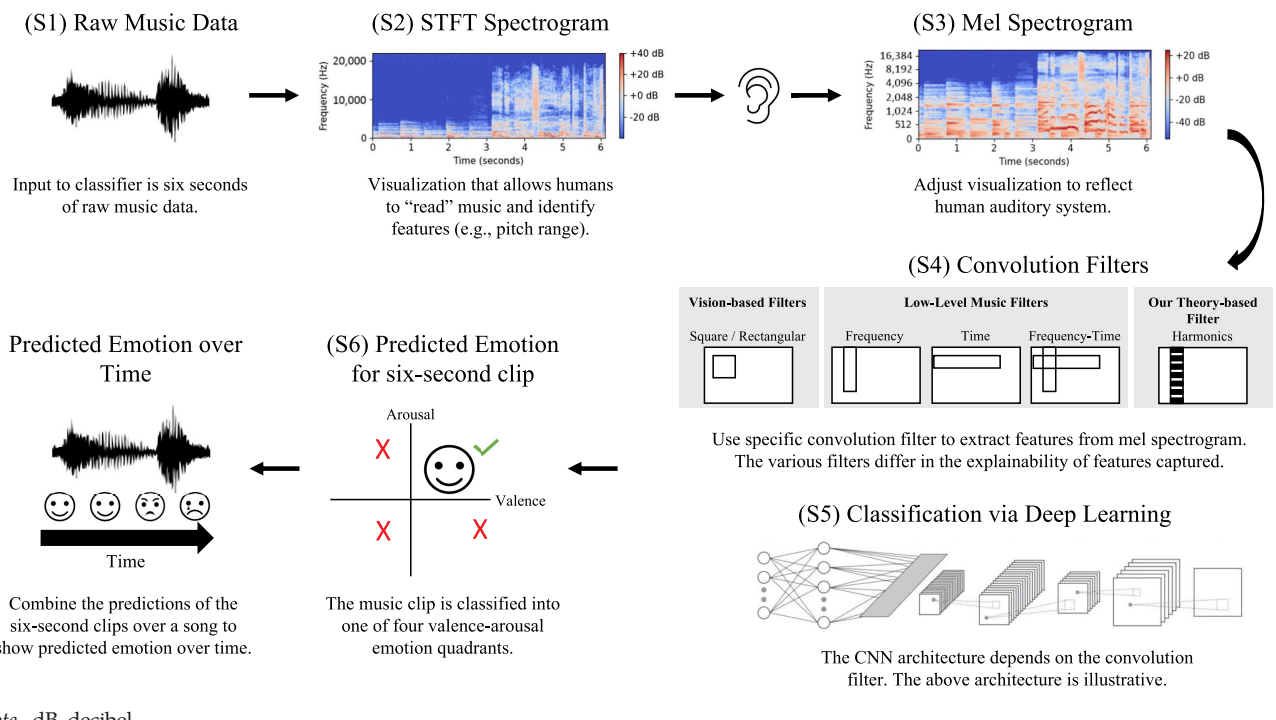
### 3.1. Model Elements

Figure 1 overviews the steps of our deep learning model that maps music to emotion. Step S1 takes six seconds of raw audio sound-wave data as input.<sup>14</sup> In Step S2, the music clip is converted to a short-time Fourier transform (STFT) spectrogram. In Step S3, we transform the STFT spectrogram to a mel spectrogram, which characterizes how the sound is perceived by the human ear. In Step S4, the mel spectrogram is used as a visual input to the CNN with one of the convolution filter types. We propose a theoretically motivated filter based on frequency harmonics to reflect aspects of music that we expect to impact listener emotion. For performance comparison, we also consider atheoretical square (and rectangular) filters that are commonly used in image processing as well as low-level music filters proposed in the literature. In Step S5, the features learned by the convolution filters from S4 are put through the remaining layers of the CNN. In Step S6, the CNN generates a classification prediction for the six-second sound clip, indicating the quadrant of the dimensional model into which the sound falls. Finally, combining the predictions of the clips shows the emotional variation over time.

**3.1.1. S1. Physical Properties of Sound Waves.** Music (or any sound) is a pressure wave that travels through the air until it reaches the listener's ear. The waveform illustrated in Step S1 of Figure 1 graphs the change in air pressure at a certain location over six seconds (Müller 2015). Audio data can be represented in a number of ways. Although a waveform is one way to visually represent sound, it does not model how humans hear sound, which is based on the underlying frequencies.<sup>15</sup>

To get to musically relevant features, we need a representation of the different frequencies that the sound wave is composed of in terms of fundamental sine waves. Sine waves determine what humans hear and are at the foundation of musical concepts, like pitch

**Figure 1.** (Color online) Music Emotion Classification Schematic



Note. dB, decibel.

and harmony. The mathematical representation of this process is the Fourier transform, which decomposes a sound wave into its constituent sine waves. Any sound wave can be represented as a combination of sine waves of different frequencies, amplitudes, and phases, known as the *partials* of the sound wave. The complete set of partials makes up the *spectrum*. Figure 2(b) shows the spectrum of the first second of music shown in the Figure 2(a) waveform. From the spectrum, we can identify the main frequencies that make up the sound and the magnitude of each frequency.

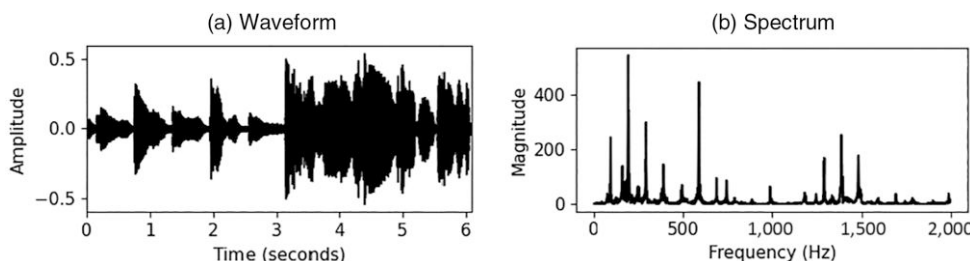
**3.1.2. S2. Short-Time Fourier Transform Spectrogram.** A spectrogram visualizes frequency and time features of audio data (Müller 2015). The STFT spectrogram, which is produced by taking the Fourier transform of short overlapping time windows of the waveform to

decompose it into its individual frequencies and their respective magnitudes, maps the squared magnitude of each frequency over time. The parameters that go into generating an STFT spectrogram are the sampling rate, window type and size, and hop length.<sup>16</sup> Let  $x$  represent the discrete-time signal of the audio signal; let  $w$  represent the window function, which takes in  $N$  samples, and let  $H$  represent the hop size. The window function specifies how we weight the audio signal within each window of time, and the hop size specifies how many samples we jump between each window. The discrete STFT  $X$  of signal  $x$  is

$$X(m, k) := \sum_{n=0}^{N-1} x(n + mH)w(n)\exp(-2\pi i kn/N), \quad (1)$$

where  $m$  is the time index,  $k \in [0 : K]$  is the frequency index, and  $i := \sqrt{-1}$ . A sampling rate of 44,100 Hz

**Figure 2.** Examples of Waveform and Spectrum



Notes. (a) Waveform of six seconds of New Soul by Yael Naim. (b) Spectrum of the first second of the waveform.

generates a spectrogram that extends up to 22,050 Hz. The STFT spectrogram can then be written as

$$S(m, k) := |X(m, k)|^2. \quad (2)$$

The magnitude of the complex number  $X(m, k)$  captures the presence of each frequency at each time sample. Squaring the magnitude yields the power of each frequency at each time sample. We generate an STFT spectrogram for each six-second clip of music. The resulting frequency  $\times$  time dimensions of the STFT spectrograms are  $2,049 \times 517$ .<sup>17</sup>

The STFT spectrogram of Figure 2(a) is represented in Figure 3(a), with the  $x$  dimension representing time, the  $y$  dimension representing frequency, and color representing the power of each frequency bin at each time sample (red (blue) is high (low) power in Figure 3(a)) online. The frequency and time dimensions are discretized because we are working with a digital signal. In the STFT spectrogram, frequency and time are shown on linear scales, whereas power is shown on a log scale and measured in decibels because humans perceive volume on a log scale.<sup>18</sup> In Figure 3(a) online, the large patch of blue before second 3 indicates a lack of high frequencies early in the music.

### 3.1.3. S3. Mel Spectrogram Based on Auditory Perception.

Humans are better at perceiving frequency differences at low pitches than at high pitches (Müller 2015).<sup>19</sup> With equal sensitivity across the frequency spectrum, the STFT spectrogram does not represent human hearing. The mel spectrogram transforms the STFT spectrogram by mapping the frequencies onto the mel scale, a log-frequency scale created to reflect human hearing. Equal distances on the mel scale have the same perceptual distance in pitch.

The additional parameter that goes into generating a mel spectrogram from an STFT spectrogram is the number of mel bands, which specifies the mel filter banks—the weights that map the STFT frequencies to the mel frequency scale. We use 256 mel bands. The mel spectrogram in Figure 3(b) more clearly displays

the differences among the lower frequencies relative to Figure 3(a).

#### 3.1.4. S4. Incorporating Harmonics-Based Structure into CNN Filter Design.

Convolution filters in CNNs are matrix operations learned from the data with the goal of correctly making predictions. In designing convolution filters to learn features to classify music emotion, we must account for how humans perceive sound and in particular, the noncontiguous structure of many musical features. We know from acoustic physics that harmonic frequencies underlie important midlevel musical features, like consonance, timbre, and pitch, which in turn, relate to emotional response. We incorporate the harmonics-based structure into the CNN filters with two goals in mind. (1) Relevant midlevel features are parsimoniously captured, and (2) the model is more explainable relative to atheoretical deep learning models. We detail the concepts of harmonics and pitch class and detail how they connect to the development of theory-based filters next.

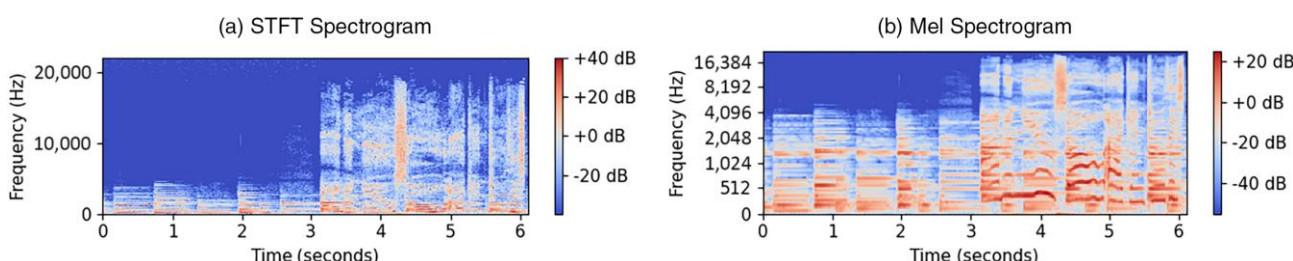
**3.1.4.1. Harmonics.** The STFT from Step S2 decomposes the sound wave into its constituent sine waves, known as partials. The harmonics of the sound wave are the partials that are integer multiples of its fundamental frequency (or lowest partial). Mathematically, the set of harmonics  $\mathcal{H} := \{\omega_n\}$  of a tone with fundamental frequency  $f_0$  contains frequencies

$$\omega_n = n f_0 \quad \forall n \in \mathbb{Z}^+. \quad (3)$$

Harmonics are the underlying reason for many musical features, and they have been referred to as the “fabric of music.”<sup>20</sup> Online Appendix C provides details on how harmonics relate to consonance, timbre, and pitch. We use the harmonics structure to motivate the design of filters to capture musical features known to impact emotion.

**3.1.4.2. Pitch Class.** We organize the harmonics-based filters around the 12 pitch classes of Western

**Figure 3.** (Color online) Spectrograms



*Notes.* (a) STFT spectrogram of six seconds of New Soul shown in Figure 2(a). The STFT spectrogram visualizes the time and frequency features of audio. The  $x$  axis represents discretized time, the  $y$  axis represents discretized frequency, and color represents the squared magnitude of each frequency bin over time. It enables one to “read” musical features, such as the range of frequencies played. (b) Mel spectrogram of six seconds of New Soul. The mel spectrogram transforms the linear frequency scale of the STFT to a log-frequency scale that reflects human auditory perception. dB, decibel.

music—A, A $\sharp$ , B, C, C $\sharp$ , D, D $\sharp$ , E, F, F $\sharp$ , G, and G $\sharp$ —because instruments are tuned to these pitch classes.<sup>21</sup> Table 1 lists the fundamental frequency of the lowest pitch in each pitch class for nearly all instruments within human hearing, and we use these frequencies to construct the filters.

**3.1.4.3. Harmonics Filter Design.** We now detail the steps to develop the harmonics-based convolution filter for a given pitch class. The unique characteristic of the filter is that it focuses on specific noncontiguous regions of the spectrogram to flexibly learn a wide variety of features. The filter uses “blinders” to select frequencies input into the CNN and a convolution size that considers a large range of frequencies at each time frame. The term “blinders” refers to the matrix operation that selects and weights the mel bands in the mel spectrogram prior to convolution, whereas “harmonics filter” refers to the combination of the blenders with convolution. Steps (i)–(v) below are done separately for each pitch class.

i. *Calculate pitch class filter frequencies.* We use the set of frequencies defined in Equation (3) to design blenders that retain only the frequencies of interest. Beginning with the lowest fundamental frequency of pitch class  $p$  in Table 1, we calculate the set of harmonic frequencies associated with  $p$ . For example, the lowest A has a fundamental frequency of  $f_0 = 27.50$  Hz, so the A harmonics  $\omega_n = nf_0$  are  $1 \times 27.50 = 27.50$  Hz,  $2 \times 27.50 = 55.00$  Hz, ...,  $801 \times 27.50 = 22,027.50$  Hz. The frequencies span the human hearing range and cover the range of the STFT spectrogram (i.e., up to 22,050 Hz).

ii. *Calculate frequency bands.* We calculate frequency bands around each  $\omega_n$ . The underlying rationale is that the human ear cannot distinguish frequencies within a small band. The exact size of the band depends on a number of factors, including duration, intensity, and frequency, so the width of the bands does not follow a rule. We calculate 1-Hz bands centered around each frequency  $\omega_n$ .

iii. *Calculate the STFT indicator column.* We identify the match between STFT bins and the frequency bands corresponding to the pitch class. To match the STFT bins with the set of frequency bands, we create an STFT indicator column such that each element is equal to one when the center frequency of the STFT bin falls within one of the frequency bands. STFT bins that are not close to the frequency bands may not be chosen.

iv. *Construct mel blenders.* We multiply the STFT indicator column by the mel filter bank to generate a mel

weight column that has  $N_{mel} = 256$  dimensions. Repeating the mel weight column over the time dimension generates the mel blenders. Finally, we multiply the mel spectrogram by the mel blenders to generate the input to the CNN’s convolution layer. Online Appendix E details the steps.

v. *Implement convolution filter.* There are a few others choices to be made before we can directly apply the convolution filter. For a spectrogram, the convolution filter height determines the number of frequency bins included, and the width determines the number of time frames. It is common practice to design the convolution filter to also have a depth (i.e., multiple channels) so that multiple features can be learned simultaneously.<sup>22</sup> The stride specifies how much the filter slides over the image before performing another operation.<sup>23</sup> Because the perception of harmonics is based on the interaction of all frequencies at any given time,<sup>24</sup> we set the filter height to the height of the spectrogram, and we set both the filter width and the stride to one time sample.<sup>25</sup> We learn filters over 8, 16, 32, and 64 channels, and we find that 32 channels performs the best for prediction; so, we set the number of channels to 32. We next apply the  $256 \times 1 \times 32$  (number of frequency bins  $\times$  number of time samples  $\times$  number of channels) convolution filter to the transformed mel spectrogram. The output of convolution on one channel is called a feature map, which is created for each channel.<sup>26</sup> We construct harmonics-based convolution filters for each of the 12 pitch classes.

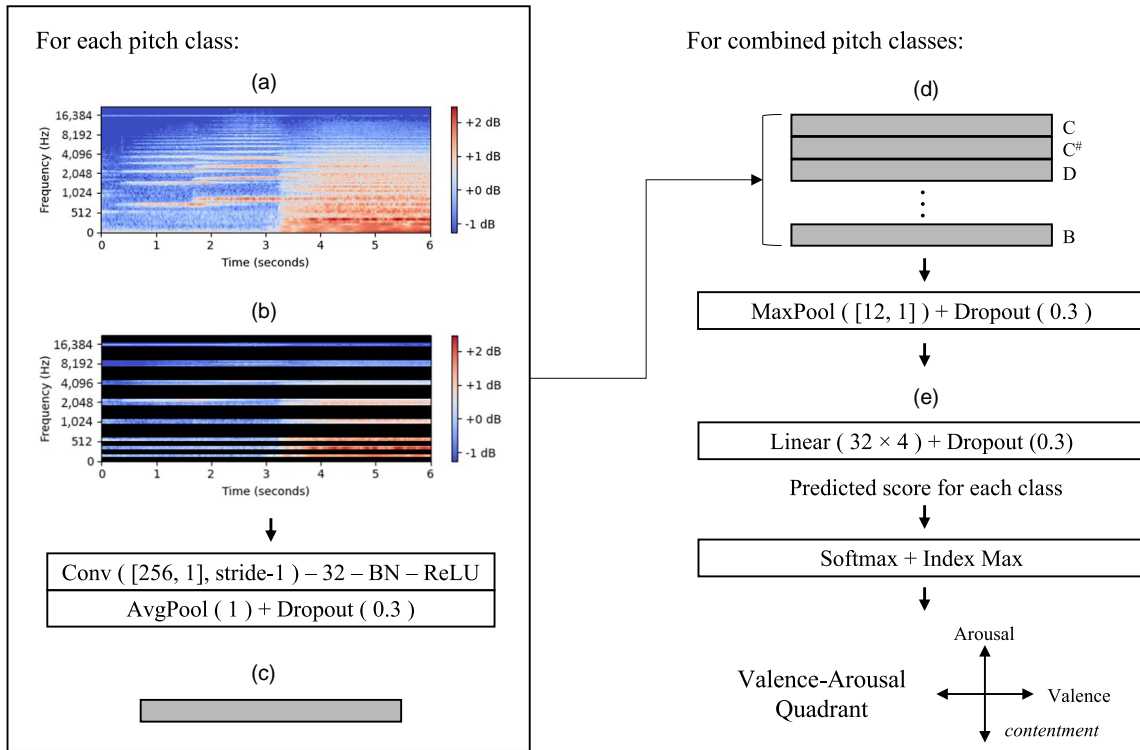
**3.1.5. S5. Convolutional Neural Network Architecture.** Our CNN to predict music emotion consists of multiple types of layers, including a convolutional layer, pooling layers, and a fully connected layer. Designing a neural network involves several architectural and hyperparameter choices. We use standard architecture choices as appropriate, and we describe the reasoning in Online Appendix F. Figure 4 summarizes the overall architecture. The operationalization of the model with harmonics filters is as follows.

1. For each pitch class,
  - a. apply the noncontiguous harmonics filters from Step S4;
  - b. batch normalize and take rectified linear unit (ReLU) of the feature maps; and
  - c. average pool over time frames and apply dropout.
2. Concatenate the hidden layers generated by each of the pitch classes.

**Table 1.** Fundamental Frequency of the Lowest Pitch in Each Pitch Class

Pitch	A	A $\sharp$	B	C	C $\sharp$	D	D $\sharp$	E	F	F $\sharp$	G	G $\sharp$
Frequency (Hz)	27.50	29.14	30.87	32.70	34.65	36.71	38.89	41.20	43.65	46.25	49.00	51.91

**Figure 4.** (Color online) Model Architecture



*Notes.* Overview of our proposed CNN architecture with harmonics filters. The input to the CNN is the mel spectrogram. For each pitch class, mel blenders are applied to place structure on what the CNN sees, and then, convolution, batch normalization (BN), ReLU, and average pooling are applied. The outputs are concatenated together and then, max pooled before going through the fully connected layer. The final output is the valence-arousal quadrant prediction. (a) Mel spectrogram input:  $256 \times 517$ . (b) Input with blenders. (c) Postconvolution layer:  $1 \times 32 \times 1$ . (d) Concatenated pitch class layers:  $12 \times 32 \times 1$ . (e) Multiclass outcome. dB, decibel.

3. Max pool over the pitch classes, and apply dropout.
4. Use one fully connected layer and apply softmax to output a probability distribution over the four emotion quadrants.
5. Output the quadrant Q1, Q2, Q3, or Q4 with max probability as the predicted label.

The emotion prediction problem aims to classify an input music clip into one of four valence-arousal quadrants (i.e., a multiclass classification problem). The objective function of the model is to minimize the cross-entropy loss between the predicted and actual outputs. The crossentropy loss  $L_{CE}$  over the set of music clips is

$$L_{CE} = -\sum_{i=1}^N \sum_{k=1}^4 y_{ik} \log(p(\hat{y}_{ik})), \quad (4)$$

where  $k$  represents the quadrant,  $y_{ik}$  represents a binary indicator for whether  $k$  is the correct class label for music clip  $i$ ,  $p(\hat{y}_{ik})$  represents the predicted probability that  $i$  is of class  $k$ , and  $N$  represents the total number of music clips. The model learns the weights that minimize the loss.

**3.1.6. S6. Predicted Emotion.** The model maps each six-second clip into a valence-arousal quadrant. Q1 captures positive valence-high arousal, Q2 captures negative valence-high arousal, Q3 captures negative valence-low arousal, and Q4 captures positive valence-low arousal. To provide a reference emotion for each quadrant, we borrow the notation from Panda et al. (2018): Q1: exuberance, Q2: anxiety, Q3: sadness, and Q4: contentment. The predictions over time characterize the dynamics of music emotion.<sup>27</sup>

### 3.2. Explainability

To gain visibility into what the model learns and uses for emotion classification, we use gradient-weighted class activation mapping. Grad-CAM uses the gradients of a target class (e.g., Q1) with respect to feature maps, which flow into a given convolutional layer, to produce a heat map that highlights the regions of the input image that *positively* predict the class (Selvaraju et al. 2017).<sup>28</sup> Because there is a filter and therefore, feature map for each pitch class, we obtain a Grad-CAM heat map for each pitch class, which is  $1 \times 517$  images (517 representing the number of time samples). The heat map

brightness value for clip  $k$  and pitch class  $p$  at each time sample  $t$  is

$$b_{kpt}^j = \text{ReLU} \left( \sum_f \alpha_f^j A_t^f \right), \text{ where } \alpha_f^j = \frac{1}{Z} \sum_t \frac{\partial y^j}{\partial A_t^f}. \quad (5)$$

In this expression,  $j$  represents the class (quadrant),  $A_t^f$  represents the feature map for channel  $f$  at time  $t$ ,  $y^j$  represents the score for class  $j$ , and  $Z$  represents the feature map size (517).<sup>29</sup> The brightness value is a linear combination of the feature maps  $A_t^f$  and their importance  $\alpha_f^j$  in predicting class  $j$ .

We stack the heat maps associated with each of the 12 pitch classes to obtain an overall heat map, in which the  $y$  axis represents the 12 pitch classes and the  $x$  axis represents time. Color denotes  $b_{kpt}^j$ , which captures the importance of the noncontiguous frequencies within each pitch class toward the classification into quadrant  $j$ , and brighter colors capture larger values. Let  $B_k^j = \sum_p \sum_t b_{kpt}^j$  represent the sum of the heat map brightness values over all pitch classes and time samples with respect to quadrant  $j$  for clip  $k$ . Let  $\bar{B}_j = (\sum_k B_k^j) / n_j$  represent the average brightness of all clips with true quadrant label  $j$ .<sup>30</sup>

Combining the structure of the harmonics filters with the Grad-CAM heat maps enables us to make sense of what the model learns and uses for classification. The harmonics filters retain frequencies relevant for a number of midlevel musical features, including consonance, which is associated with the presence of harmonic combinations of frequencies. Consonance is of particular importance for music emotion, and so, we expect not only the filters to learn consonance but also, consonance to play an important role and contribute significantly to emotion classification. Recall that consonance is associated with positive valence and low arousal, whereas dissonance is associated with negative valence and high arousal (Gabrielsson 2016). Because brightness in the heat maps (i.e.,  $b_{kpt}^j$ ) summarizes the positive contribution of all the harmonic frequencies (by pitch class) at a given time to the classification of the target class, we expect high brightness for Q4 and low brightness for Q2. In other words, we expect brightness in the heat maps to capture consonance. To assess whether the model learns consonance and uses it for classification, we form two sets of hypotheses regarding the brightness of the Grad-CAM heat maps based on music theory.

First, for a single clip, we expect consonant parts of the clip to have high brightness with respect to Q4 (i.e.,  $b_{kpt}^4$ ) because consonance is associated with Q4. On the flip side, consonant parts of the clip should have low brightness with respect to Q2 (i.e.,  $b_{kpt}^2$ ) because dissonance is associated with Q2 (Gabrielsson and Lindström 2010). We expect the brightness with respect to Q1 and Q3 to be between those of Q2 and Q4. Second, across

clips in each quadrant, we expect that for a given level of arousal, positive valence clips (based on the true labels) should on average have brighter heat maps than negative valence clips because consonance is associated with positive valence. Similarly, for a given level of valence, low-arousal clips should on average have brighter heat maps than high-arousal clips because consonance is associated with low arousal (Gomez and Danuser 2007). We, therefore, expect to observe the following pattern:  $\bar{B}_1 > \bar{B}_2, \bar{B}_4 > \bar{B}_3, \bar{B}_4 > \bar{B}_1$ , and  $\bar{B}_3 > \bar{B}_2$ . We assess these hypotheses in Section 4.3.

Finally, given that consonance would separate out Q4 (high) and Q2 (low), the remaining issue is how the model separates Q1 and Q3. For this, we look at the features learned by the model that are the most important for classification into the quadrants. The learned features correspond to the outputs from the convolutional layer (postmax pooling) that are input to the fully connected layer (the input to panel (e) in Figure 4). More specifically, we examine whether the learned features most important in predicting Q1 and Q3 correlate to musical features associated with harmonics known to be able to differentiate arousal levels (Online Appendix C). In Section 4.3, we find the learned features to be connected to roll-off, spectral centroid, and spectral skewness. High arousal is associated with the presence of higher harmonics and higher pitch, which correspond to higher roll-off, higher spectral centroid, and lower spectral skewness. Having identified these features predictive of arousal, we expect learned features positively correlated with roll-off and spectral centroid and learned features negatively correlated with spectral skewness to be positively correlated with the likelihood of a Q1 classification and negatively correlated with the likelihood of a Q3 classification.

### 3.2.1. Benchmark Deep Learning Models for Comparison.

We train several benchmark deep learning models for comparison. The models can be characterized as either atheoretical or musically motivated and focused on low-level features. In contrast to our model, these models only focus on contiguous regions of the spectrogram.

The atheoretical models include CNN with  $(n \times n)$  square filters or with rectangular filters, both tall and skinny ( $2n \times n$ ) and short and wide ( $n \times 2n$ ). These are borrowed from image recognition models as in Krizhevsky et al. (2012). CNNs with square filters have been fine-tuned to reflect how we see and recognize images, but these models do not represent how we hear and process audio. Therefore, square filters are atheoretical from the perspective of acoustic physics. Square filters capture some audio features, but it is unclear what these are and how they relate to music emotion. Compared with square filters, rectangular filters of different shapes might allow us to capture features that span a larger

portion of the frequency space or a larger portion of the time space.

The musically motivated models that focus on low-level features include CNN models with filters designed to extract either frequency or time features, first proposed by Pons et al. (2016). Tall and skinny ( $a \times 1$ ) filters are designed to capture timbral features across the frequency spectrum (e.g., a specific combination of notes), whereas short and wide ( $1 \times b$ ) filters are designed to capture temporal features (e.g., tempo). Pons et al. (2016) apply these ideas to ballroom genre classification, and they find that, individually, these filters do not perform as well as a CNN with square filters but that combining the two types of filters with an additional fully connected layer results in comparable performance. We provide additional implementation details for the benchmark models in Online Appendix D.

We note that our CNN model with harmonics filters is more parsimonious than the benchmark deep learning models. Although our model has 100,000 trainable parameters, the CNNs with square and rectangular filters have nearly 5 million and 10 million parameters, respectively. The CNN with frequency filters has 1.5 million parameters, the CNN with time filters has 2.2 million parameters, and the CNN with frequency-time filters has 3.8 million parameters. With the additional structure, the harmonics filters learn features relevant to emotion recognition as effectively as others models but with fewer parameters (as we show in Section 4.2). As described earlier, this has advantages in generalizability and robustness.

## 4. Empirical Analysis

We begin by describing the data sets used to train the models. We then report the performance of our proposed architecture with harmonics filters and compare it against the benchmark models proposed in the literature. Finally, we show how our model is explainable using gradient-based model visualizations and compare it with visualizations generated by other CNN models, which use atheoretical and low-level filters.

### 4.1. Data Sets

We combine two public data sets compiled by music emotion researchers, and they serve complementary purposes in our analysis: Soundtracks (Eerola and Vuoskoski 2011) and the MediaEval Database for Emotional Analysis in Music (DEAM) (Aljanaki et al. 2017).

The Soundtracks data set consists of 360 excerpts from movie soundtracks that range in duration from 10 to 30 seconds. One benefit of movie soundtracks is that they are composed to elicit emotion. The music clips are instrumental and do not contain any lyrics, dialogue, or sound effects. The clips were chosen to (1) either elicit a discrete emotion or be high or low on valence, arousal,

or tension, (2) evoke only a single emotion over the length of the clip, and (3) be unfamiliar to prevent song familiarity from impacting emotion tagging. University students and staff with musical expertise annotated the song emotions, and six annotators tagged each music excerpt.<sup>31</sup> Perceived discrete emotions, valence, and arousal were separately annotated on a scale from one to seven. Interrater consistency (Cronbach's alpha) was 0.92 for valence, 0.90 for arousal, and ranged from 0.66 to 0.93 for the discrete emotions. We split the excerpts into nonoverlapping six-second segments. Excerpts selected for the discrete emotions happy, sad, tender, fear, and anger are mapped onto the valence-arousal quadrants such that happy maps to Q1, fear and anger map to Q2, sad maps to Q3, and tender maps to Q4. The excerpts selected for the dimensional emotions and surprise are converted to the four quadrants by discretizing the valence-arousal space around the midpoint (4, 4). All six-second clips from the same excerpt have the same quadrant label because these excerpts were chosen to only evoke a single emotion over the length of the clip.

The DEAM data set consists of 1,802 mostly 45-second excerpts of royalty-free music. The music annotations were crowdsourced through MTurk, and each excerpt was annotated by at least 10 workers. Perceived valence and arousal were annotated on a scale from -10 to 10 every half second using a graphical interface. The clips were largely unfamiliar to workers. Interitem consistency (Cronbach's alpha) was 0.28–0.66 for arousal and 0.20–0.51 for valence. In contrast to Soundtracks, the DEAM music was not chosen to elicit a particular emotion, which helps to explain the relatively low annotation consistency.<sup>32</sup> In addition, the DEAM music can vary in emotion over time. DEAM complements Soundtracks by covering more of the valence-arousal space. We include the classical and pop music genres from DEAM because these genres conform to Western music theory. We divide each clip into nonoverlapping six-second segments and average the 12 annotations taken every half second to obtain valence-arousal labels. To convert the continuous valence-arousal labels to the four quadrants, we discretize the valence-arousal space around the midpoint (0, 0). We thus obtain the same Q1–Q4 quadrants across both data sets.

Finally, we combine Soundtracks and DEAM. Additional details are provided in Online Appendix G. To improve data balance across the quadrants, we subsample the data so that no quadrant has more than 50% more clips than any other. In total, we have 2,019 six-second music clips distributed as 28%, 19%, 28%, and 24% over Q1, Q2, Q3, and Q4, respectively.

### 4.2. Model Performance

We use precision, recall, and  $F_1$  score, standard measures in the machine learning literature, to evaluate our model. We calculate these metrics for each class

(quadrant), and a weighted average by the number of samples in each class determines each overall measure. Table 2 summarizes the performance of the models. The performance metrics are averaged over each fold of the held-out test data from stratified 10-fold cross-validation.<sup>33</sup> The standard deviations of the performance measures over the 10 folds are in parentheses.

In evaluating the performance of the model, it is important to recognize that performance benchmarks for classification using deep learning models can vary significantly by prediction task because of differences in difficulty levels. For example, in a data set of images of cats and dogs, it might be relatively easy to identify the animal type (cat/dog), but it might be more difficult to identify other labels, like age, using the same images. Prediction tasks involving *subjective human response* (e.g., emotion recognition and humor detection) typically have lower prediction accuracy than more *objective* recognition tasks (e.g., object identification and instrument identification). An important reason is that for subjective tasks, without objective ground truth, humans have heterogeneous responses, implying less agreement on the “ground truth” (Davani et al. 2022). In such cases, even our best approximation is bounded above by this subjectivity. Music emotion is a challenging classification problem because it is highly subjective.

**Table 2.** Classification Performance—Deep Learning Models

Filter type	Precision	Accuracy/recall	$F_1$
Atheoretical filters			
Mel—square	0.5160 (0.0568)	0.5003 (0.0538)	0.4841 (0.0663)
Mel—tall rectangle	0.5067 (0.0808)	0.5014 (0.0590)	0.4809 (0.0784)
Mel—wide rectangle	0.5232 (0.0617)	0.4911 (0.0442)	0.4774 (0.0585)
Theory-based low-level filters			
Mel—time	0.3597 (0.1055)	0.3717 (0.0768)	0.3186 (0.0890)
Mel—frequency	0.5501 (0.0730)	0.4806 (0.0532)	0.4703 (0.0592)
Mel—time-frequency	0.5058 (0.0801)	0.4827 (0.0656)	0.4622 (0.0771)
Proposed theory-based midlevel filters			
Mel—harmonics	0.5224 (0.0505)	0.5049 (0.0478)	0.5057 (0.0506)

Notes. Precision =  $\frac{\text{True Positive}}{\text{Predicted Positive}}$ . Recall =  $\frac{\text{True Positive}}{\text{Actual Positive}}$ .  $F_1 = \frac{2 \times \text{Precision} \times \text{Recall}}{\text{Precision} + \text{Recall}}$ . Precision is particularly useful when false positives are costly (e.g., spam detection). Recall is particularly useful when false negatives are costly (e.g., disease detection). Accuracy is equivalent to weighted average recall and captures the proportion of correct predictions out of the entire set of data.  $F_1$  is useful when we want a balance between precision and recall. The measures are weighted by the proportion in each quadrant.

Thus, our model performance should be compared with benchmarks within the class of prediction problems seeking to predict subjective human response. Examples include humor detection (Chen and Lee 2017 obtain an  $F_1$  of 0.61, with chance guessing at 0.51) and moral foundation classification (Pavan et al. 2023 obtain an  $F_1$  of 0.45, with chance guessing at 0.19). We note that even though instrument identification and music emotion classification both use music as input data, instrument identification typically has much higher levels of performance.<sup>34</sup>

First, we detail the classification performance of the benchmark deep learning models, which use atheoretical and low-level filters. The CNNs with atheoretical square and rectangular filters obtain  $F_1$  values of around 0.48. Although a low-level CNN filter based on time alone does not perform as well as the atheoretical filters, frequency filters perform almost as well as the atheoretical filters. The combination of time and frequency filters performs comparably with the model using only frequency filters, suggesting that frequency-related features play a larger role in eliciting emotion in short music clips relative to temporal features.

Next, we examine the performance of our proposed theory-based midlevel CNN filters that account for harmonics. We find that this model obtains an  $F_1$  of 0.51,<sup>35</sup> which is no worse than the best benchmark models,<sup>36</sup> as well as comparable precision and recall measures.<sup>37</sup>

Overall, the CNN that uses the harmonics filters performs as well as those using atheoretical filters, despite having far fewer parameters. The key distinction is that in contrast to the atheoretical filters, our proposed harmonics filters directly connect to theoretical concepts that help explain what the model learns and uses for emotion classification.

### 4.3. Model Explainability

We now compare the explainability based on Grad-CAM for our CNN model with harmonics filters and other benchmark CNN models.

**4.3.1. Explainability of Harmonics Filters.** In Section 3, we discussed the patterns to expect in terms of the brightness of Grad-CAM heat maps based on theory related to harmonics, perception of consonance, and emotional response to consonance. We illustrate explainability around the role of consonance in two ways. First, we compare the heat maps with respect to all four quadrants for a single clip labeled to be in the high-consonance Q4 quadrant. We expect consonant parts of the clip to have high brightness with respect to Q4 and low brightness with respect to Q2. Second, we consider eight distinct out-of-sample clips—two for each of the four quadrants. We expect to see the average ordering of brightness to follow the relative ordering

discussed earlier. In addition, we calculate the average brightness of all out-of-sample clips for each quadrant (i.e.,  $\bar{B}_j$ ).

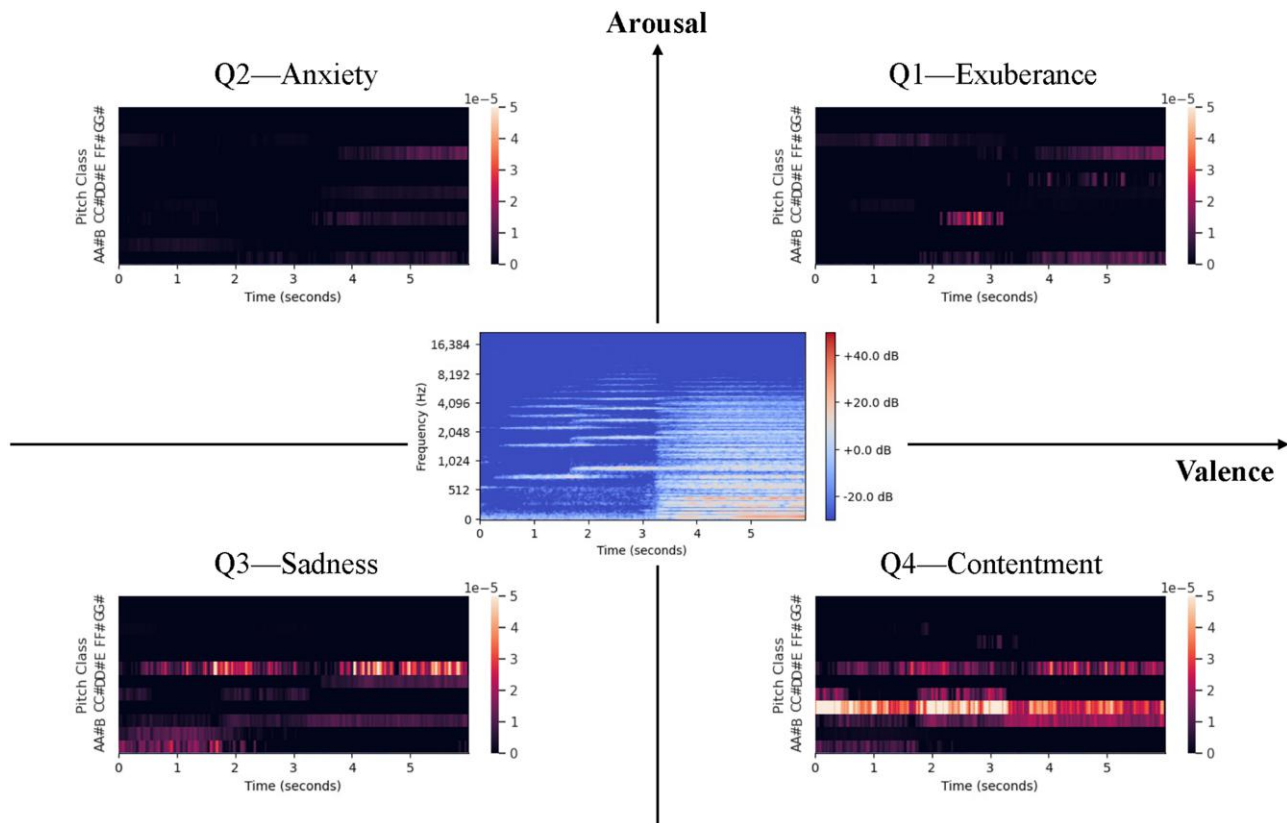
First, we look at the heat maps of a Q4 music clip that we know begins with only frequencies that follow a harmonic pattern and is, therefore, consonant. The center panel in Figure 5 shows the mel spectrogram of a Q4 clip that begins with a violin playing one note, changing notes, and then, being joined by additional instruments shortly after three seconds. We know that playing a single violin string produces a harmonic sound, which can be seen in the parallel horizontal bars at frequencies that are integer multiples of approximately 740 Hz between 0.25 and 2.5 seconds (e.g., 740, 1,480, and 2,220 Hz) and multiples of 880 Hz between 1.75 and 3.25 seconds (e.g., 880, 1,760, and 2,640 Hz). In the Grad-CAM heat maps, the portions of the clip with harmonic frequencies light up brightly for Q4, indicating that these frequencies most greatly contribute to the Q4 classification but not for Q2. The Q1 and Q3 heat maps have some points of brightness but not as many as Q4 or as few as Q2. Overall, the Q4

heat map is much brighter than the other heat maps. These patterns are consistent with what we would expect to see based on theory if the model learns and uses consonance for emotion classification.

Second, we analyze the heat maps for different music clips for which the model made the same prediction as the true label. Figure 6 shows a few prototypical Grad-CAM heat maps and their associated mel spectrograms. These heat maps come from clips in the hold-out sets from 10-fold crossvalidation. In general, we observe patterns in line with theory in that positive valence heat maps are brighter than negative valence heat maps and that low-arousal heat maps are brighter than high-arousal heat maps.

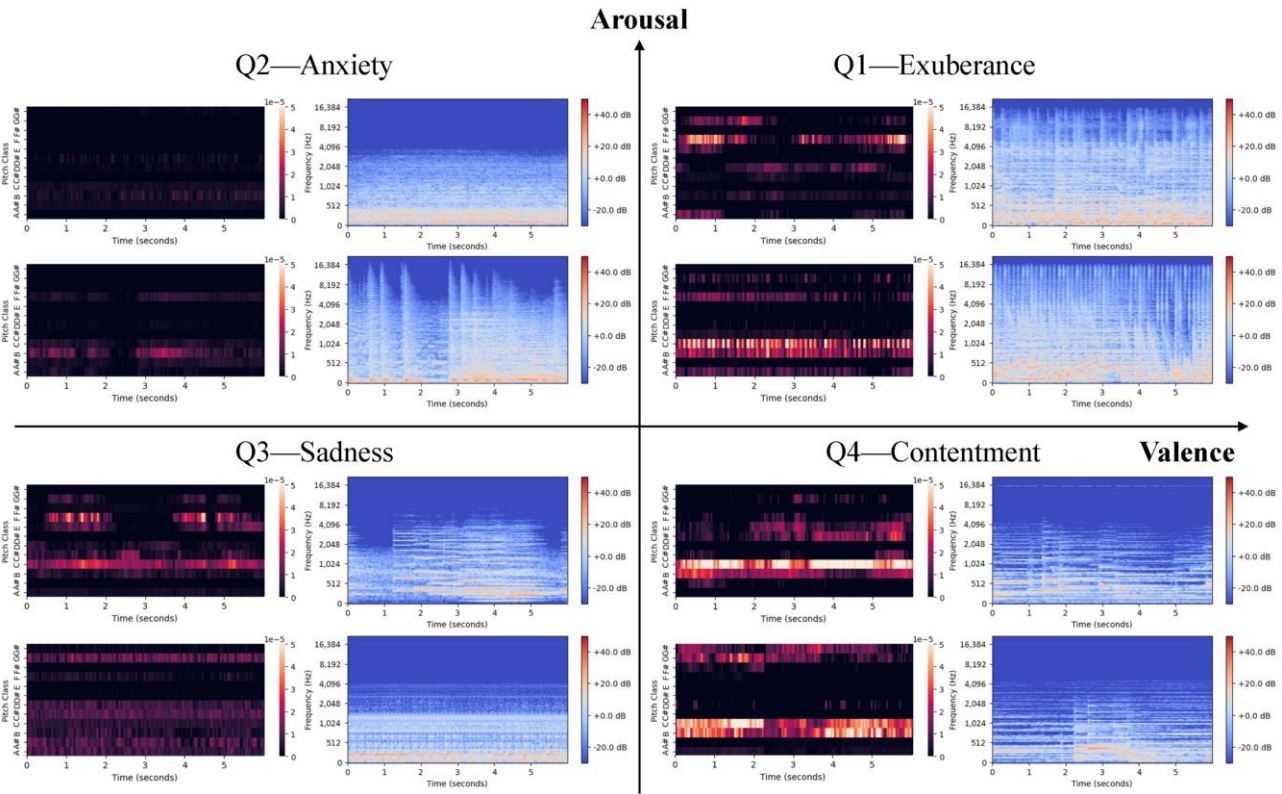
When we quantify the heat map brightness across all of the clips for the hold-out sets, we find that the scaled average brightness values based on the true emotion labels are  $\bar{B}_1 = 53$ ,  $\bar{B}_2 = 45$ ,  $\bar{B}_3 = 62$ , and  $\bar{B}_4 = 72$ . The average brightness observed per quadrant is consistent with our hypothesized ordering (i.e.,  $\bar{B}_1 > \bar{B}_2$ ,  $\bar{B}_4 > \bar{B}_3$ ,  $\bar{B}_4 > \bar{B}_1$ ,  $\bar{B}_3 > \bar{B}_2$ ), further supporting the consonance-based interpretation of the Grad-CAM heat maps.<sup>38</sup>

**Figure 5.** (Color online) Harmonics Grad-CAM Heat Maps of a Q4—Contentment Clip over Quadrants



*Notes.* The center panel is the mel spectrogram of Soundtracks track 183, seconds 0–6. The images in the four quadrants correspond to the Grad-CAM heat maps for the classification of the clip into the four emotion quadrants using the CNN model with harmonics filters. The music clip starts off with a violin, producing a harmonic sound that can be seen in the mel spectrogram through the parallel horizontal bars at frequencies that are integer multiples of approximately 740 and 880 Hz. The Q4 heat map shows that 0.25–3.25 seconds most greatly contribute to the Q4 classification, which corresponds to periods of overlapping harmonics and consonance. The Q2 heat map shows that this same period does not positively contribute to the Q2 classification. This pattern suggests that brightness in the heat maps captures consonance.

**Figure 6.** (Color online) Harmonics Grad-CAM Heat Maps by Quadrant



*Notes.* Within each emotion quadrant, the right panels are mel spectrograms of music clips, and the left panels are their Grad-CAM heat maps. The following six-second clips are shown: Q1: DEAM song 1,811, seconds 27–33 and DEAM song 1,892, seconds 21–27; Q2: Soundtracks song 216, seconds 6–12 and Soundtracks song 142, seconds 0–6; Q3: DEAM song 2,012, seconds 39–45 and DEAM song 159, seconds 27–33; and Q4: Soundtracks song 33, seconds 12–18 and Soundtracks song 48, seconds 6–12. dB, decibel.

Explainability builds trust in the model by providing transparency that the model learns patterns consistent with theory rather than picking up spurious correlations, like discussed in the wolf versus husky example from Ribeiro et al. (2016) in Section 1. The heat maps highlight areas of consonance, a midlevel feature related to noncontiguous frequencies that is generally not observable by eye, and the patterns of brightness align with the expected relationship between consonance and emotion.<sup>39</sup>

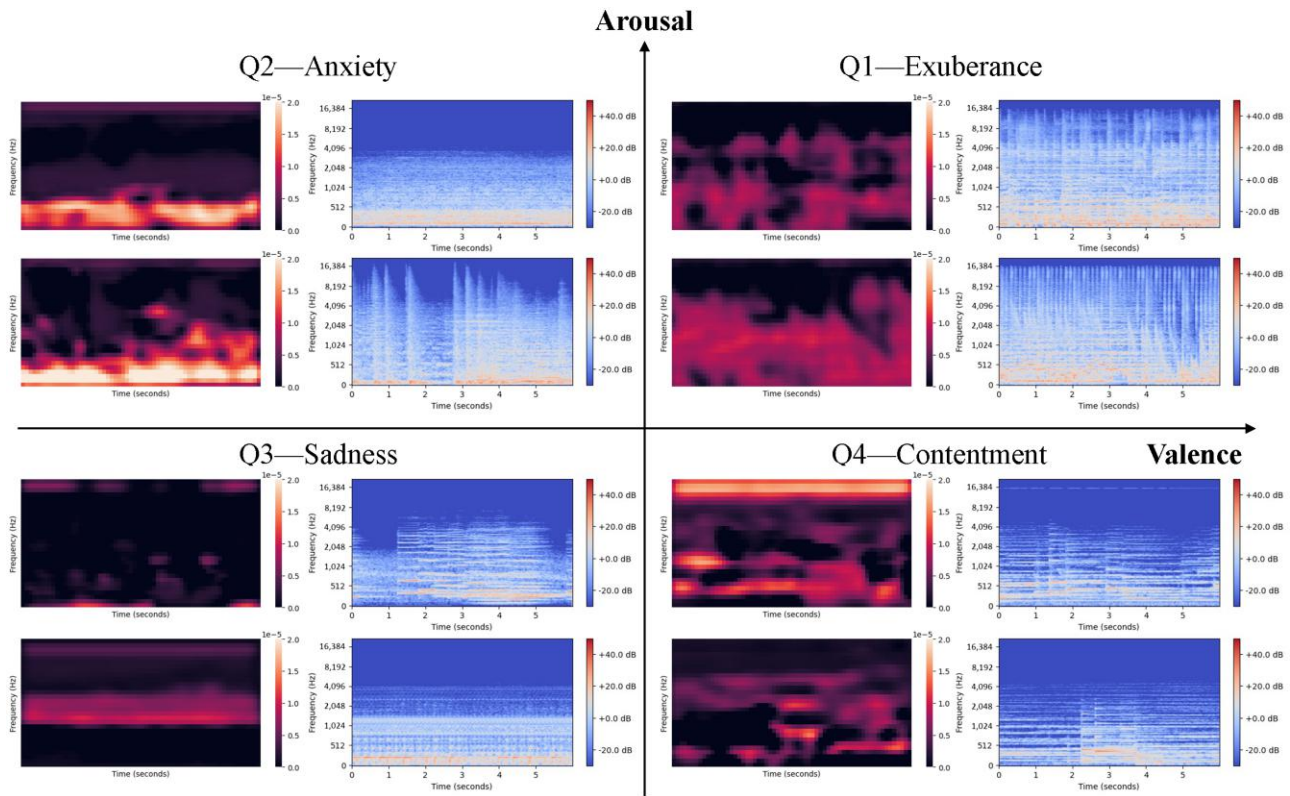
On the separation between Q1 and Q3, the results are overall consistent with our predictions in Section 3.2. We obtain the features that are the most influential in the classification of a music clip into Q1 and Q3 based on SHAP values.<sup>40</sup> The correlations between the two most important learned features for classifying both Q1 and Q3 and musical features known to differentiate arousal are 0.35 and −0.41, respectively, for roll-off; 0.32 and −0.36, respectively, for spectral centroid; and −0.32 and 0.44, respectively, for spectral skewness. As discussed earlier, the first feature should then be positively correlated with Q1 and negatively correlated with Q3, and the second feature should be negatively correlated

with Q1 and positively correlated with Q3 because Q1 is associated with high arousal and Q3 is associated with low arousal. We assess this; as expected, we find that the first learned feature is positively correlated with Q1 (0.45) and negatively correlated with Q3 (−0.47) and that the second learned feature is negatively correlated with Q1 (−0.47) and positively correlated with Q3 (0.51). Thus, being able to separate out high and low arousal helps differentiate between Q1 and Q3.

#### 4.3.2. Limited Explainability of Atheoretical and Low-Level Filters.

Grad-CAM visualizations can also be produced for the other filter types. We find that given their low-level focus without specific theory to guide our expectations, it is more difficult to interpret what musical features are captured and connect how they contribute to the classification of a particular class. The Grad-CAM heat maps for the square filter CNN in Figure 7 are equivalent to heat maps produced for an image recognition model. They show which contiguous regions of the input image contribute to the classification of a particular class, providing an idea of the range of frequencies and times contributing to the classification.

**Figure 7.** (Color online) Square Grad-CAM Heat Maps by Quadrant



*Notes.* Within each emotion quadrant, the right panels are mel spectrograms of music clips, and the left panels are their Grad-CAM heat maps. The clips are the same as those shown in Figure 6. The bright portions of a heat map capture the parts of the mel spectrogram that most greatly contribute to the classification of the specified emotion. The heat map covers the dimensions of the final feature map after convolution. The x axis captures time, and the y axis captures frequency. dB, decibel.

However, it is unclear what human-understandable musical features are being learned. Note that in contrast to our harmonics filters, pitch classes are not used here.

The heat maps based on separate time and frequency filters highlight which time periods or frequencies contribute most to a particular classification (see Online Appendix Figure K1). Similar to square filters, it is less clear how to interpret the heat maps, making it challenging to understand what musical features the models learn. In the models using atheoretical and low-level filters, it is more challenging to determine what musical feature is learned and used for emotion classification. Thus, our contribution in incorporating the noncontiguous theory-based harmonics filters is to provide greater explainability, specifically with consonance, while obtaining similar performance as atheoretical filters.

#### 4.4. Model Capability to Learn Features

Although our discussion of explainability has primarily focused on a specific and important feature (i.e., consonance), harmonics filters can also learn other features as foreshadowed in Section 4.3. For instance, the combination of harmonic frequencies provides information about pitch perception, timbre (or tone color), and

spectral spread and complexity (McAdams and Giordano 2015).

The comparable classification accuracy between the theory-based CNN with harmonics filters and the models with atheoretical filters suggests that the harmonics filters are learning multiple musical features relevant for emotion classification because consonance alone would not yield such high accuracy. To assess this systematically, we check whether classification performance improves if we add handcrafted features found to predict music emotion. Some handcrafted features, like mel frequency cepstral coefficients, are more atheoretical in that they were not designed for music but instead, were designed for speech. Other features, like tempo, are more theory based in that they were designed with music in mind. Limited improvement in performance would suggest that the model with harmonics filters captures information similar to the handcrafted features. In addition, we assess the correlations between the features learned by the harmonics filters and the handcrafted features. High correlations would suggest that the learned features capture information similar to the handcrafted features.

First, we train two random forest (RF) models using only handcrafted features to show the baseline

Downloaded from informs.org by [192.31.236.2] on 12 September 2024, at 07:08 . For personal use only, all rights reserved.

performance of the features. Random forest is an ensemble learning method known to be both robust and accurate. For music emotion prediction, Unni et al. (2022) found that random forest provided the best accuracy over a number of machine learning models. The first model uses MFCCs, which have proven successful in music classification, including genre and emotion classification (Kim et al. 2010). We use 13 MFCC coefficients as well as their first and second derivatives, resulting in 39 features. The second model uses 11 handcrafted features highlighted by Panda et al. (2018) for their ability to predict the four emotion quadrants; we name the set of features the Top Handcrafted Features, and Online Appendix Table I1 summarizes them.<sup>41</sup>

Next, we combine the handcrafted features with the features learned by our deep learning model that uses harmonics filters. We extract the learned features before the final classification step. We then concatenate these learned features with the handcrafted features and input this combination to a random forest model to make the final classification. This allows us to test whether the handcrafted features are redundant to the learned features. Another advantage of this approach is that we retain explainability while being able to add handcrafted features.

Table 3 shows that the inclusion of MFCCs or the Top Handcrafted Features marginally improves predictive performance relative to using only the deep learning model ( $F_1$  of 0.53 versus 0.51). This suggests that the harmonics filters do not capture all of the information in the handcrafted features but do capture information similar to many of the handcrafted features. When we assess the correlations between the learned features and the handcrafted features, we observe reasonably high values ranging from -0.41 to 0.45 for tone color-related features. This is in line with our expectations because tone color relates to frequency rather than time, and our harmonics filters are specifically designed around frequency. We further find that combining the features

learned by the harmonics filters with two time-related handcrafted tempo features improves predictive performance more.

Overall, the results suggest that our theory-based deep learning model learns not only features that capture similar information to the Top Handcrafted Features but also, additional features useful for predicting emotion. One advantage of the deep learning model is that each feature does not have to be specifically engineered. However, there is still some value in incorporating handcrafted features related to time.

## 5. Application: Emotion-Based Ad Insertion in Content Videos

Our proposed theory-based deep learning model can be used in a number of real-time *emotion-based* applications by predicting the valence and arousal of music clips. We demonstrate the value with an illustrative application involving emotion-based contextual targeting, where the algorithm determines the optimal emotion-based ad insertion point for a video ad within a content video (e.g., YouTube video) with time-varying emotional content.

Such emotion-based contextual targeting with automated content matching is gaining importance. Increasing privacy restrictions limit person-specific targeting of advertising, making contextual and content-based targeting for ad placement more relevant and useful.<sup>42</sup> Further, given the vast amount of user-generated content available, nonalgorithmic approaches to matching ads with content are challenging, if not impossible, to implement at scale. The size of the matching problem is very large, and a platform like YouTube needs to match billions of ads and content videos daily.

Throughout a content video, emotion often varies over time, and so, the various ad insertion slots differ in emotion. Because ads also often elicit emotion, we seek to understand how to match the ad to the insertion slot

**Table 3.** Classification Performance—Incorporating Handcrafted Features

Features	Model	Precision	Accuracy/recall	$F_1$
Benchmark models with handcrafted features				
MFCCs	RF	0.4764 (0.0419)	0.4716 (0.0446)	0.4615 (0.0459)
Top Handcrafted Features	RF	0.4559 (0.0637)	0.4563 (0.0576)	0.4513 (0.0615)
Combined theory-based midlevel filters + handcrafted features				
Mel—harmonics + MFCCs	CNN + RF	0.5376 (0.0525)	0.5278 (0.0483)	0.5236 (0.0491)
Mel—harmonics + Top Handcrafted Features	CNN + RF	0.5361 (0.0633)	0.5294 (0.0606)	0.5259 (0.0605)
Mel—harmonics + Tempo features	CNN + RF	0.5407 (0.0537)	0.5329 (0.0493)	0.5295 (0.0493)

based on emotion. Although marketing researchers have considered the overall emotion of content videos for ad matching (Kamins et al. 1991, Coulter 1998, Puccinelli et al. 2015, Kapoor et al. 2022), our focus is on automatically identifying the optimal ad insertion slot within videos that vary in emotion over time.

### 5.1. Does Emotional Congruence or Contrast Work Better for Ad Insertion?

It is an empirical question as to whether ads that are similar to the emotional context of the content video increase or decrease ad attention and memorability. Some behavioral studies have found that emotional congruence is more effective (Lee et al. 2013), including studies of matching in persuasion and fluency (Teeny et al. 2021). However, other studies have found that consumers have a preference for positive stimuli when feeling negative emotions (Andrade 2005) and that perceptual contrast draws attention, suggesting that emotional contrast may be more effective. To answer this empirical question, we conduct a laboratory experiment in which we exogenously insert ads into content videos at different insertion points. We characterize each ad and each insertion point by their respective emotions, which are based on human tagging. This allows us to create a measure of emotional distance between each ad and each insertion point. We measure ad skip and brand recall, and we see whether and how emotional distance influences these ad engagement measures.

Next, after identifying the more effective ad matching strategy, we evaluate whether our proposed theory-based deep learning model can select emotionally appropriate ads based on predicted emotion relative to benchmark models. Given that our focus is on music and its effects, we treat the emotion evoked by the background music of the video as a proxy for the emotion evoked by the overall video.<sup>43</sup> We also examine the impact of nonmusic-based emotion in videos. In this setting of automated contextual targeting, the explainability of our model would increase managerial trust in the tool to make reasonable decisions that generalize across a range of different content videos and ads outside of the initial training setting and thus, increase confidence in adopting it.

### 5.2. Experiment: Is Emotional Congruence or Contrast More Effective?

We discuss the experimental design and results below.

**5.2.1. Experimental Setup.** There are multiple ad insertion points, which vary in evoked emotion, within each content video. The outcome variables of interest are ad skip (as a proxy for attention and interest) and brand recall (as a proxy for memorability). We use a full factorial design across four ads, four content videos, and six

ad insertion points per content video, yielding a total of 96 experimental cells.

We develop a Qualtrics survey that shows an ad inserted partway through a content video, mimicking the concept of YouTube's midroll ads. Similar to YouTube, a "Skip Ad" button appears six seconds into the ad, allowing participants to skip the remainder of the ad. Upon watching the ad to completion or skipping it, the content video picks up where it left off. Each participant sees only one content video and only one ad. After watching the content video, participants are asked questions about the content video and the ad.

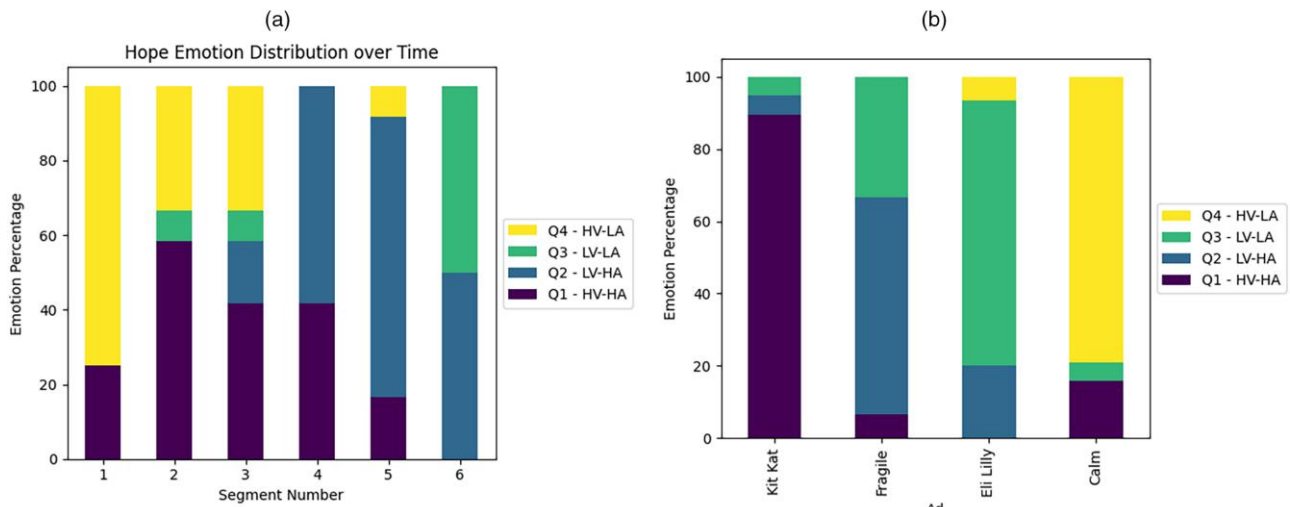
**5.2.2. Content Videos and Ads.** We select a diverse set of content videos and ads. The content videos are selected to (a) contain background music most of the time and (b) be long enough to vary in emotion over time and allow for multiple ad insertion points. The videos range from 5.7 to 7.9 minutes in length, include both animated and live-action videos, and include videos with and without speech. Online Appendix Table L1 provides details on the four content videos. For each content video, we fix six ad insertion points (time 1, ..., 6) that are roughly one minute apart and occur at natural changes in the audio and images, similar to YouTube.<sup>44</sup> Online Appendix Table L2 specifies the insertion times.

We select four ads such that each of the four valence-arousal quadrants is represented by the primary emotion in the first six seconds of one of the ads. The emotion of the first six seconds is important because viewers on YouTube have the option to skip at six seconds. We seek to understand the interaction effect of the content video emotion with the initial ad emotion. The ads include background music, are 30 seconds long, and cover a range of industries.<sup>45</sup> Online Appendix Table L3 provides details on the four ads.

**5.2.2.1. Emotion Tagging.** Because we seek to measure emotional distance, we must first characterize the emotion of the content videos and ads. Within the experiment, we use human-tagged emotion as the ground truth. To obtain the emotion tags, we recruit survey participants on Prolific, an online survey platform. We show respondents either the content videos in segments (as defined in Online Appendix Table L2) or the first six seconds of the ads and ask them about their valence and arousal levels after watching each clip.<sup>46</sup> With multiple tags per clip, each clip can then be characterized by the distribution of emotion over the quadrants.

Figure 8(a) shows the emotion distribution over video segments for the content video titled Hope. Viewers largely felt positive (Q1 and Q4) during the first three segments, high arousal (Q1 and Q2) during segment 4, anxious during segment 5 (Q2), and negative (Q2 and Q3) during segment 6, demonstrating a large variation

**Figure 8.** (Color online) Human-Tagged Emotion



Notes. (a) Content over time. (b) Ads. HV, high valence; LV, low valence; HA, high arousal; LA, low arousal.

in emotion over time. Online Appendix Figure L1 shows the emotion distributions of all four content videos.

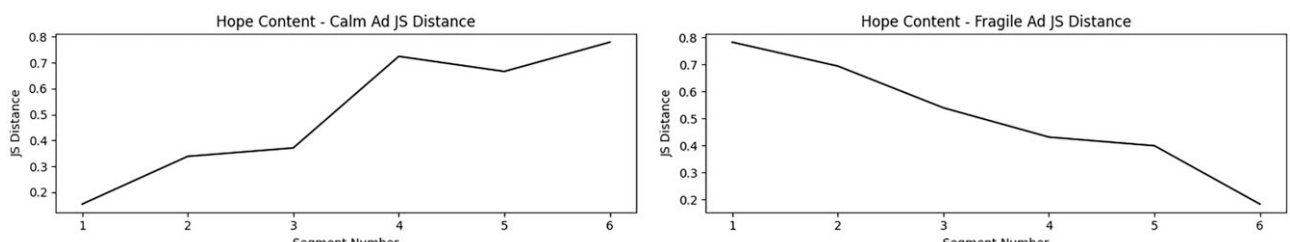
Figure 8(b) displays the emotion distributions of the first six seconds of each ad. As can be seen, the four ads were selected so that each emotion quadrant would be represented.

**5.2.3. Emotional Distance Measure.** To measure emotional distance between an ad and an insertion point in the content video, we calculate the Jensen–Shannon (JS) distance. The JS distance is computed between their probability distributions over the emotion quadrants. Let  $P_t$  represent the emotion probability distribution of the content video at time  $t$ , and let  $Q$  represent the emotion probability distribution of the ad. JS distance is defined as

$$JSD(P_t||Q) = \sqrt{\frac{1}{2}D(P_t||M) + \frac{1}{2}D(Q||M)}, \quad (6)$$

where  $M = 1/2(P_t + Q)$  and  $D$  is the Kullback–Leibler (KL) divergence. The benefits of JS distance over KL divergence are that it is symmetric between  $P_t$  and  $Q$

**Figure 9.** JS Distance Between Content Video and Ads



and that it is always finite. The larger the JS distance, the more dissimilar the ad emotion is from the content video emotion at time  $t$ .

Figure 9 plots the JS distances between the content video Hope and the two ads Calm and Fragile Childhood across Hope's six insertion points (or segments). For Calm, the minimum distance (i.e., the greatest emotional similarity) occurs after segment 1, and the maximum distance (i.e., the greatest emotional contrast) occurs after segment 6. However, for Fragile Childhood, the opposite occurs. Online Appendix Figure L2 plots the JS distances of the 16 potential combinations of content videos and ads. These plots show that there is large variation in emotional distances between the ads and the content videos. The JS distances in the data range from 0.017 to 0.783.

**5.2.4. Outcomes of Interest.** Our dependent variables are “revealed preference”-type metrics and of significant interest to advertisers. Ad skip captures whether someone skips or voluntarily continues to watch the ad. Unaided brand recall captures whether someone paid attention to the ad and its memorability.

An ad skip occurs if the participant presses the “Skip Ad” button within five seconds of its appearance.<sup>47</sup> This definition captures the emotion interaction of the content video at the time of ad insertion and the first six seconds of the ad. We capture recall in the set of questions asked to participants after watching the content video. In the survey, the brand shows as video information when the ad begins and disappears after three seconds. Therefore, even if participants skip the ad, they are still exposed to the brand.

**5.2.5. Experimental Results.** Each participant is randomly assigned to 1 of the 96 cells.<sup>48</sup> Across all content videos, ads, and insertion points, 1,413 participants on average skipped 42.0% of ads (viewed 58.0%) and correctly recalled 45.2% of brands. As expected, the correlation between skip and recall is negative, with a value of  $-0.23$  ( $p < 0.01$ ).

To determine the impact of emotional distance on skip and recall, we regress a binary indicator for skipping (or a binary indicator for correctly recalling) on JS distance, controlling for covariates. We estimate the following regression equation:

$$f(y_{ijt}) = \alpha + \beta JS D_{ijt} + \gamma X_{ijt} + \epsilon_{ijt}, \quad (7)$$

where the outcome  $y_{ijt}$  represents a skip indicator or a correct recall indicator for ad  $i$  at insertion point  $t$  within content video  $j$ ,  $JS D_{ijt}$  represents the JS distance between the emotion of the content video at point  $t$  and the ad,  $X_{ijt}$  represents covariates (i.e., ad, content, and time of insertion point), and  $\epsilon_{ijt}$  represents the error term.

For ease of interpretation, we assume a linear probability model for skip and recall, and we report the least squares coefficients in Table 4. The results retain the same signs and levels of statistical significance when we assume a logit model. Columns (1) and (4) in Table 4 do not include any covariates. We find that greater emotional distance increases the probability of skipping and decreases the probability of recalling the brand.

**Table 4.** Effect of Emotional Distance on Ad Engagement

Outcome	<i>I(Skip)</i>			<i>I(Recall)</i>		
	(1)	(2)	(3)	(4)	(5)	(6)
<i>JS Distance</i>	0.188** (0.075)	0.196** (0.078)	0.206*** (0.079)	-0.179** (0.077)	-0.166** (0.077)	-0.168** (0.077)
<i>Time</i>		0.001*** (0.001)	0.001*** (0.001)		-0.001 (0.001)	-0.001 (0.001)
<i>Time</i> <sup>2</sup>			-0.001 (0.001)			0.001 (0.001)
Content FE	No	Yes	Yes	No	Yes	Yes
Ad FE	No	Yes	Yes	No	Yes	Yes
<i>R</i> <sup>2</sup>	0.004	0.035	0.036	0.003	0.092	0.092

Notes. There were 1,413 observations for all regressions; robust standard errors are used. FE, fixed effect.

\*\* $p < 0.05$ ; \*\*\* $p < 0.01$ .

Columns (2) and (5) in Table 4 include content video fixed effects, ad fixed effects, and a linear time trend for ad insertion time because the times differ across content videos. The results remain robust to including these covariates. Finally, columns (3) and (6) in Table 4 include a second-order polynomial in time, and the results do not qualitatively change.<sup>49</sup> Taken altogether, the JS distance coefficients suggest that emotional congruence between the ad and the insertion point is more effective than emotional contrast for ad engagement.

### 5.3. Ad Insertion Automation

Our theory-based and benchmark models can predict the emotion distributions of the ads and content to calculate emotional distances at scale. We use these to compare ad skip and recall outcomes from showing each ad at the most emotionally similar ad insertion point based on the predictions of the models.

**5.3.1. Calculating Model-Predicted Emotional Distances.** We transform the first 6 seconds of audio of each ad and the 30 seconds of audio before each ad insertion point in the content videos into mel spectrograms. For the content videos, we break the 30-second clips into five 6-second clips. We use the models to predict the emotion distribution of each six-second clip.<sup>50</sup> For the 30-second content video clips, we average over the five predicted emotion distributions associated with each 6-second clip. Using the 24 content emotion distributions (four content videos  $\times$  six insertion points) and the 4 ad emotion distributions, we calculate the JS distances between the ads and the content at the six insertion points. For each combination of the model, content video, and ad, we determine which ad insertion point is the most emotionally similar.<sup>51</sup>

**5.3.2. Skip and Recall Rates.** From the experiment, we have the skip and recall rates for the 96 experimental cells. For each model, we average the skip and recall

**Table 5.** Ad Insertion Automation Results

Feature	Model	JS distance	Skip rate, %	Recall rate, %
Atheoretic filters				
Mel—square	CNN	0.510	42.0	45.7
Mel—tall rectangle	CNN	0.450	43.5	47.3
Mel—wide rectangle	CNN	0.419	44.5	45.1
Theory-based low-level filters				
Mel—time	CNN	0.437	40.9	46.6
Mel—frequency	CNN	0.466	46.9	45.9
Mel—time-frequency	CNN	0.446	44.3	48.6
Proposed theory-based midlevel filters				
Mel—harmonics	CNN	0.429	42.0	48.9
Mel—harmonics + Tempo features	CNN + RF	0.395	40.7	48.8

rates as well as the ground-truth JS distances (based on human tagging) of the most emotionally similar insertion point for each of the four ads in each of the four content videos as predicted by each model, and we show the results in Table 5. Note that these average skip and recall rates are based on a simulation of ad insertion automation using the experimental data.

Our proposed theory-based model using harmonics filters selects insertion points that are relatively high in emotional similarity (i.e., low JS distance) compared with the other deep learning models. These ad insertion points generate relatively favorable skip and recall rates, suggesting that our model can be useful in automated emotion-based ad insertion. The models that includes tempo features, the best-performing model from Section 4.4, further improve upon these results.

**5.3.3. Incorporating Other Video Modalities.** Our primary analysis has focused on using emotion evoked from music. However, with videos, emotional content may be present across multiple modalities (e.g., facial expressions and text of speech). Multimodal emotional content can also be used to predict emotional distance. When the videos have human faces, we can use publicly available tools to estimate emotion from facial expressions. Similarly, emotional content can also be obtained from voice tonality and speech text.

In our application, we observe that speech or human faces might not be present in each content video or in the first six seconds of ads, implying that using speech or facial emotion is not always feasible. For the videos with human faces, we assess the skip and recall rates when including face emotion alongside music emotion. We could not include speech emotion because there was not enough speech in the first six seconds of the ads. We find mixed evidence of the value of including face emotion. Including face emotion slightly improves the recall rate but hurts the skip rate. Online Appendix L.1 details the analysis.

Overall, we find that there is potential in incorporating emotion information from images and text, but the

existing tools are limited in their ability to extract emotion information from short clips (i.e., the first six seconds of ads) and animated videos. However, this is a moving target, and as these methods steadily improve, these findings could well change.

#### 5.4. Managerial Implications

Past studies have provided evidence that emotional ads impact attention and memory (Holbrook and Batra 1987, Cohen et al. 2018). The results of this study support the theory that emotional similarity decreases ad skipping and increases brand recall. Our method can be used to determine time-varying emotion based on the background music of videos, and we show that it performs as well as atheoretical CNN models while being explainable.

We demonstrate the value of our model in a video advertising setting by mapping music to emotion to determine the optimal emotion-based insertion point within a content video. In practice, we expect emotion to be used as a complement to other ad targeting variables.

Our proposed model could also be useful in a number of other applications. For example, existing Spotify playlists built around a unifying emotion are based on the overall emotion of a song. However, one quarter of songs are skipped in the first five seconds, so the interaction of the ending of one song and the beginning of the next is a critical point for a listener's decision to continue with a playlist.<sup>52</sup> Our model can quantify the emotional match between the end of one song and the beginning of the next to allow for continuity (or contrast) in the listener's emotional experience. The classifier can also be used in contexts that match music with other forms of unstructured data. For example, a text classifier can be used for a news article, whereas our model can be used for the video ad. More broadly, any setting that involves emotion and requires music choice (e.g., call-waiting music) could benefit from a music emotion classifier.

#### 6. Conclusion

Our research contributes to the literature that studies consumer response to music, which represents one type

of unstructured data. Music is pervasive in customer interactions with firms. From music in ads to hold music for call centers and from workout playlists to background music in retail stores, customers engage with music in a variety of ways. The exponential growth of user-generated content has created a huge quantity of high-dimensional data, and automated prediction of music-evoked emotion at scale can be helpful for a variety of marketing decisions. However, unlike other unstructured data, such as text (e.g., Toubia et al. 2021, Wang et al. 2022), images (e.g., Liu et al. 2020, Dew et al. 2022, Huang et al. 2022, Troncoso and Luo 2023, Zhang and Luo 2023, Sisodia et al. 2024), and video (e.g., Yang et al. 2021, Chakraborty et al. 2024), music has received relatively little attention in the marketing literature.

We develop a CNN to classify the emotion evoked by music. Our framework integrates a number of theoretically motivated elements to develop harmonics-based filters, combining the physics of music and human hearing of sound as well as human perception of music. Our approach achieves similar classification performance to that of atheoretical models. In terms of explainability, we exploit specific elements of music theory to construct filters capable of capturing consonance. We visualize the model's prediction process using Grad-CAM, which provides a visual representation of the areas in an image (spectrogram for sound) that contribute the most to the classification into a particular target class. Although this provides a degree of transparency, we note that making deep learning models more explainable is an active area of research in machine learning. Finally, we use our music emotion classifier in an application where we match the time-varying emotion in a content video with the emotion of the first six seconds of an ad, and we show that it performs as well as benchmark models while being more explainable.

We conclude with a discussion of some limitations and suggestions for future research. First, we focus on relatively short music clips in our data and model. This choice is motivated by the application of ad insertion, where typically, a video ad is played and the user is allowed the choice to skip six seconds into the ad. Although the method in principle applies to clips of any duration, in practice we might consider altering the architecture of the deep learning model to include temporal dependencies. Second, incorporating listener heterogeneity based on demographics could further improve the model's predictive accuracy, but given privacy concerns, we have opted to leave out listener data. Third, investigating the complementarity of unstructured high-dimensional data across modalities would be valuable. In sum, we believe that the growing variety of data in conjunction with explainable models offers rich research opportunities to quantify emotion and its impact.

## Acknowledgments

All authors certify that they have no affiliations with or involvement in any organization or entity with any financial interest or nonfinancial interest in the subject matter or materials discussed in this manuscript.

## Endnotes

<sup>1</sup> A content analysis of over 3,000 ads showed that 94% of ads use music (Allan 2008). Further, over 75% of advertising hours in broadcast media use music in some form (Huron 1989). As Huron (1989, p. 572) states, “on a second-for-second basis, advertising music is the most meticulously crafted and most fretted about music ....”

<sup>2</sup> As of 2024, YouTube has 2.49 billion users, spending on average 49 minutes per day on YouTube. Spotify has 615 million users whose playlists span over 100 million tracks.

<sup>3</sup> Many researchers have adopted the valence-arousal framework for music emotion classification (e.g., Yang and Chen 2011, Panda et al. 2018). Our model can also easily be adapted for other emotion frameworks, such as the discrete emotion framework.

<sup>4</sup> The theory-based filters are distinct from handcrafted features (e.g., mel frequency cepstral coefficients (MFCCs)) that are used with traditional machine learning models (e.g., support vector machine) because the filter operations are learned from the data rather than predefined.

<sup>5</sup> See Online Appendix Table A1 for music definitions.

<sup>6</sup> In 2020, McKinsey conducted a survey that found that explainability is among the top risks that firms are concerned about regarding artificial intelligence models. The source for this information is at <https://www.mckinsey.com/business-functions/quantumblack/our-insights/global-survey-the-state-of-ai-in-2020>.

<sup>7</sup> We use the emotion elicited by only the music as a proxy (or the dominant modality) for the emotion elicited by the video. This is reasonable given that music is typically designed to elicit the intended emotion in videos (Bullerjahn and Güldenring 1994, Herget 2021). We also examine how other modalities in video (e.g., text of dialogues and images) can be used alongside music emotion in Section 5.3.3.

<sup>8</sup> More specifically, it is a two-dimensional image in which the *y* axis denotes frequency, the *x* axis denotes time, and color captures the magnitude of each frequency at each time point.

<sup>9</sup> Goodfellow et al. (2016, p. 309) write in their textbook the following about square convolution filters: “When a task involves incorporating information from very distant locations in the input, then the prior imposed by convolution may be inappropriate.”

<sup>10</sup> Consonance refers to a combination of notes that sound pleasant when played simultaneously. Dissonance, or the lack of consonance, refers to a combination of notes that sound jarring when played simultaneously (Müller 2015). Consonance is one of the few features that has a strong relationship with valence. Models that predict music emotion have historically been better at classifying arousal and worse at classifying valence (Aljanaki et al. 2017).

<sup>11</sup> Online Appendix Table B1 organizes features used in music classification by level of interpretability.

<sup>12</sup> Nelson et al. (2013, p. 90) write: “Most films, however, are targeted at a broad, global audience with the implicit understanding that they share a common familiarity with Western tonal music, so the overtone series is the foundation of the cinematic musical language.” According to Christensen (2006), “tonality most often refers to the orientation of melodies and harmonies toward a referential (or tonic) pitch class.”

<sup>13</sup> For a survey focused on television advertising, see Wilbur (2008).

<sup>14</sup> We use six seconds of audio, but the model can easily be adapted to incorporate other audio lengths.

<sup>15</sup> Two different waveforms can map to the same sound.

<sup>16</sup> To operationalize this procedure, we first digitize the analog audio signal by sampling from the signal because we are working with digital technology. The sampling rate represents the number of samples taken per second and is measured in hertz. The optimal sampling rate depends on the context. We will use a sampling rate of 44,100 Hz, which is also used for CD recordings because it generates an STFT spectrogram that covers the range of human hearing, spanning from roughly 20 to 20,000 Hz. Because time has been discretized, we now measure time in terms of the number of samples rather than in seconds. We set the window type to Hann, the window size to 4,096 samples, and the hop length to 512 samples. These are standard choices in the literature (Müller 2015). A Hann window is a bell-shaped window that places more weight on the center of the window and less weight on the edges of the window.

<sup>17</sup> We follow the literature in choosing the dimensions of the spectrogram (Müller 2015). The time dimension is equal to the length of music clip (6 seconds)  $\times$  sampling rate (44,100 Hz)/hop length (512) =  $(6 \times 44,100/512) = 517$ . The frequency dimension is equal to half the window sample size + 1 =  $(4,096/2 + 1) = 2049$ . The rationale for using half the window sample size is that in transforming the audio information from the time domain to the frequency domain, the discrete Fourier transform transforms the 4,096 samples to 4,096 frequency bins, but half of them are redundant. It is helpful to have high granularity on the frequency dimension because our theory-based convolution filters are focused on frequency. We observed empirically that using 4,096 frequency bins outperforms 2,048 frequency bins.

<sup>18</sup> By using a log scale, small intensity values of relevance are visible to a human reader.

<sup>19</sup> Pitch is a subjective measure of frequency, and it is defined as the attribute of sound that allows it to be ordered on a scale from low to high. For a pure tone sine wave, the pitch and frequency are the same, and they are determined by its fundamental or lowest frequency. However, they can differ for more complex and realistic sounds. In all cases, the higher the frequency, the higher the perceived pitch is.

<sup>20</sup> The source is <https://splice.com/blog/what-are-harmonics/>.

<sup>21</sup> In Western music, instruments are typically tuned in reference to A4 being 440 Hz to establish typical intervals between instruments.

<sup>22</sup> If height and width represent the  $y$  and  $x$  axes, channel can be thought about as the  $z$  axis. The loss function incentivizes the model to learn different features over different channels. So, for example, for images, one channel might learn to detect vertical edges, a second channel might learn to detect horizontal edges, and a third channel might learn to detect texture. The optimal number of channels is determined empirically. The flexibility to learn different features is a large part of why CNNs have been so successful in image classification.

<sup>23</sup> A small stride captures more fine-grained information but also requires more computational and resource costs.

<sup>24</sup> In earlier versions of the model, we tried other window lengths and did not find improved predictive performance. We also tried combining filter types, but similarly, we did not see an increase in performance; so, we chose the most parsimonious model and did not include other filter types.

<sup>25</sup> Recall that the mel spectrogram has 517 time samples, which are a function of the music clip length, the sampling rate, and the hop length used to construct the spectrogram.

<sup>26</sup> This convolution transforms the  $256 \times 517$  mel spectrogram to a  $1 \times 517$  feature map for each channel.

<sup>27</sup> Because music is temporal, it is natural to think about using a model that captures dependencies over time. Note, however, that our interest is in classifying emotion for short audio clips, so it is not clear that long-range dependencies will help with predictive performance. An alternative architecture is to incorporate positional information by including an recurrent neural network (RNN) layer in place of average pooling to summarize the feature maps over time. We find that this model results in lower classification performance ( $F_1 = 0.42$ ) than our proposed model without positional encoding. This is consistent with the fact that in Choi et al. (2017, figure 3), they also find that RNN marginally reduces the classification accuracy for the two emotions they classify (happy and sad). Because of the short duration of six seconds, there is limited potential to improve performance, and the overall performance from adding the RNN deteriorates because of overfitting because the RNN introduces many more parameters. However, including RNN may improve performance with longer duration clips. Note also that in our setting, the emotion of a song may vary over time, so it might not be the case that longer duration clips would always perform better, especially if we are making an assumption that a single clip has only one dominant emotion.

<sup>28</sup> For example, when classifying an image as a great white shark as opposed to a whale shark, a good image classifier might produce a heat map that highlights the area with sharp teeth.

<sup>29</sup> This equation is adapted from Selvaraju et al. (2017, equations 1 and 2) to our setting, where the feature maps for each channel have only one dimension. ReLU takes the max of zero and the input to the function.

<sup>30</sup> The number of clips with true quadrant label  $j$  is  $n_j$ .

<sup>31</sup> Music emotion researchers group emotion into expressed, perceived, and evoked emotion. Expressed emotion refers to the emotion that the performer tries to communicate, perceived emotion refers to the emotion that a listener perceives from a song, and evoked emotion refers to the emotion that a listener actually feels in response to a song (Jaquet et al. 2014). Most often, the emotion of interest is evoked emotion, but because of its subjectivity, researchers typically build data sets that use perceived emotion labels, as is the case for Soundtracks and DEAM. Perceived emotion and evoked emotion are typically positively related (Kallinen and Ravaja 2006), so we do not distinguish between the two.

<sup>32</sup> The relatively low Cronbach's alpha also highlights the inherent subjectivity of music emotion labeling.

<sup>33</sup> We create the folds at the song level rather than at the six-second clip level to prevent data leakage. If clips from the same song are part of both the training data and the testing data, the training process may pick up some other elements of the song that can be used to predict emotion in the test data, leading to high accuracy but lower generalizability.

<sup>34</sup> For instrument identification, trained ears will have high agreement on which instruments are present, and predicting instruments obtains high  $F_1$  values, from 0.82 for guitar to 0.99 for drums (Blaszke and Kostek 2022). For emotion classification, Liu et al. (2017) obtain  $F_1$  values ranging from 0.41 to 0.60 on the CAL500 and CAL500exp data sets.

<sup>35</sup> Online Appendix J shows the confusion matrices for the square and harmonics filters.

<sup>36</sup> An alternative input to the mel spectrogram is the STFT spectrogram. Although the literature has most frequently used mel spectrograms because they are more reflective of how humans hear, we also assess the performance of using STFT spectrograms because they are more granular. We find that the average mel model performance measures are slightly higher than those from the STFT spectrograms.

<sup>37</sup> In Online Appendix H, we show the effect of data set size on model performance. We subsample the data and show the change

in precision, recall, and  $F_1$  for the model with harmonics filters. As expected, we find that more data improve performance, but consistent with Brigato and Iocchi (2021), even very small data sets provide signal to differentiate among classes.

<sup>38</sup> When we average the brightness values by predicted label, we observe the same ordering. In this case, the scaled average brightness levels are  $\bar{B}_1 = 55$ ,  $\bar{B}_2 = 42$ ,  $\bar{B}_3 = 45$ , and  $\bar{B}_4 = 90$ .

<sup>39</sup> Although we can get a sense of concepts, like tempo, loudness, and timbre, by reading a mel spectrogram, we cannot visually extract consonance (except in rare cases, such as a single violin string being played). Music theorists have proposed several formulas to quantify sensory dissonance based on human hearing and the physics of sound. Our filters enable the deep learning algorithm to learn this relationship as it relates to listener emotion.

<sup>40</sup> SHAP values measure feature importance, capturing the contribution of each feature to the model's output.

<sup>41</sup> Panda et al. (2018) comprehensively consider a wide set of hand-crafted features, and they identify the ones that most impact classification into the emotion quadrants. Most of the identified features are low-level features that capture tone color/timbre.

<sup>42</sup> Many web browsers have eliminated third-party cookies. In March 2021, Google announced that it would stop tracking the web-browsing behavior of individuals (source: <https://www.businessinsider.com/google-to-stop-tracking-individuals-web-browsing-precision-ad-targeting-2021-3>).

<sup>43</sup> Film professionals and researchers recognize the importance of music in driving emotion. Nelson et al. (2013, p. 79) write: "Music plays many roles in film, but it is possible to categorize all of them into two primary functions: creating consonance or dissonance to highlight the film's emotion or narrative."

<sup>44</sup> From YouTube's documentation, "YouTube's advanced machine learning technology looks over a large volume of videos and learns to detect the best places for midrolls. This is done by evaluating factors like natural visual or audio breaks" (source: <https://support.google.com/youtube/answer/6175006?hl=en&zippy=%2Cfrequently-asked-questions>).

<sup>45</sup> For ads originally longer than 30 seconds, we use a 30-second clip to keep the ad length consistent across cells. In these cases, we start and end the ads at natural points.

<sup>46</sup> Each content video received 12–17 tags, and each ad received 15–19 tags. Valence and arousal are measured on a scale of 0 to 100, so we convert the valence and arousal levels to valence-arousal quadrants.

<sup>47</sup> This is different from YouTube's definition of skip rate (i.e., 1 – view rate). YouTube counts a view as having watched at least 30 seconds of an ad or its duration if it is less than 30 seconds.

<sup>48</sup> Participants were asked to watch a five- to eight-minute video and then answer some questions about the video. The survey was limited to Prolific workers who have U.S. citizenship, are fluent in English, have an approval rating greater than 97%, and have completed at least 50 previous Prolific tasks. Workers who tagged the content video and ad emotions were excluded from participating in the experiment. The survey took on average 11.6 minutes to complete, and each participant was paid \$1.80 for the time. Participants who failed the attention checks were excluded.

<sup>49</sup> We also assess the impact of emotional distance on log view time, and we find that the regression coefficients are negative and statistically significant at the 0.05 level. We focus on skip because we are interested in understanding the interaction of the content video and the beginning of the ad, for which ad skip is a better proxy.

<sup>50</sup> For the deep learning models, the final softmax layer generates a probability distribution over the four valence-arousal quadrants.

Instead of selecting the highest probability quadrant, we retain the probability distribution.

<sup>51</sup> For example, we find that for the content video Hope and ad Fragile, the mel—harmonics model suggests that the sixth ad insertion point is the most emotionally similar to the ad.

<sup>52</sup> See <https://www.theguardian.com/music/2014/may/07/one-quarter-of-spotify-tracks-are-skipped-in-first-five-seconds-study-reveals>.

## References

- Aljanaki A, Yang YH, Soleymani M (2017) Developing a benchmark for emotional analysis of music. *PLoS One* 12(3):e0173392.
- Allan D (2008) A content analysis of music placement in prime-time television advertising. *J. Advertising Res.* 48(3):404–417.
- Andrade EB (2005) Behavioral consequences of affect: Combining evaluative and regulatory mechanisms. *J. Consumer Res.* 32(3):355–362.
- Belanche D, Flavián C, Pérez-Rueda A (2017) Understanding interactive online advertising: Congruence and product involvement in highly and lowly arousing, skippable video ads. *J. Interactive Marketing* 37(1):75–88.
- Blaszke M, Kostek B (2022) Musical instrument identification using deep learning approach. *Sensors* 22(8):3033.
- Boughanmi K, Ansari A (2021) Dynamics of musical success: A machine learning approach for multimedia data fusion. *J. Marketing Res.* 58(6):1034–1057.
- Brigato L, Iocchi L (2021) A close look at deep learning with small data. *2020 25th Internat. Conf. Pattern Recognition (ICPR)* (IEEE, Piscataway, NJ), 2490–2497.
- Bruner GC (1990) Music, mood, and marketing. *J. Marketing* 54(4):94–104.
- Bullerjahn C, Güldenring M (1994) An empirical investigation of effects of film music using qualitative content analysis. *Psychomusicology* 13(1–2):99–118.
- Chakraborty I, Chiong K, Dover H, Sudhir K (2024) Can AI and AI-Hybrids detect persuasion skills? Salesforce hiring with conversational video interviews. *Marketing Sci.* Forthcoming.
- Chen L, Lee CM (2017) Convolutional neural network for humor recognition. Preprint, submitted February 8, [https://www.researchgate.net/publication/313519600\\_Convolutional\\_Neural\\_Network\\_for\\_Humor\\_Recognition](https://www.researchgate.net/publication/313519600_Convolutional_Neural_Network_for_Humor_Recognition).
- Choi K, Fazekas G, Sandler M, Cho K (2017) Convolutional recurrent neural networks for music classification. *2017 IEEE Internat. Conf. Acoustics Speech Signal Processing (ICASSP)* (IEEE, Piscataway, NJ), 2392–2396.
- Choi K, Fazekas G, Cho K, Sandler M (2018) A tutorial on deep learning for music information retrieval. Preprint, submitted May 3, <https://arxiv.org/abs/1709.04396>.
- Chowdhury S, Vall A, Haunschmid V, Widmer G (2019) Toward explainable music emotion recognition: The route via mid-level features. Preprint, submitted July 8, <https://arxiv.org/abs/1907.03572>.
- Christensen T (2006) *The Cambridge History of Western Music Theory* (Cambridge University Press, Cambridge, UK).
- Cohen JB, Pham MT, Andrade EB (2018) The nature and role of affect in consumer behavior. Jansson-Boyd CV, Zawisza MJ, eds. *Routledge International Handbook of Consumer Psychology* (Routledge, London), 306–357.
- Corrigall KA, Schellenberg EG (2013) Music: The language of emotion. *Handbook of Psychology of Emotions: Recent Theoretical Perspectives and Novel Empirical Findings*, vol. 2 (Nova Hauppauge, New York), 299–325.
- Coulter KS (1998) The effects of affective responses to media context on advertising evaluations. *J. Advertising* 27(4):41–51.
- Davani AM, Diaz M, Prabhakaran V (2022) Dealing with disagreements: Looking beyond the majority vote in subjective annotations. *Trans. Assoc. Comput. Linguistics* 10:92–110.

- Dew R, Ansari A, Toubia O (2022) Letting logos speak: Leveraging multiview representation learning for data-driven branding and logo design. *Marketing Sci.* 41(2):401–425.
- Errola T, Vuoskoski JK (2011) A comparison of the discrete and dimensional models of emotion in music. *Psych. Music* 39(1):18–49.
- Frade JLH, de Oliveira JHC, Giraldi JdME (2021) Advertising in streaming video: An integrative literature review and research agenda. *Telecomm. Policy* 45(9):102186.
- Fu Z, Lu G, Ting KM, Zhang D (2010) A survey of audio-based music classification and annotation. *IEEE Trans. Multimedia* 13(2):303–319.
- Gabrielsson A (2016) The relationship between musical structure and perceived expression. Hallam S, Cross I, Thaut M, eds. *The Oxford Handbook of Music Psychology*, 2nd ed. (Oxford University Press, Oxford, UK), 215–232.
- Gabrielsson A, Lindström E (2010) The role of structure in the musical expression of emotions. Juslin PN, ed. *Handbook of Music and Emotion: Theory, Research, Applications* (Oxford Academic, Oxford, UK), 367–400.
- Gerg ID, Monga V (2021) Structural prior driven regularized deep learning for sonar image classification. *IEEE Trans. Geoscience Remote Sensing* 60:1–16.
- Gomez P, Danuser B (2007) Relationships between musical structure and psychophysiological measures of emotion. *Emotion* 7(2):377–387.
- Goodfellow I, Bengio Y, Courville A, Bengio Y (2016) *Deep Learning*, vol. 1 (MIT Press, Cambridge, MA).
- Goodrich K, Schiller SZ, Galletta D (2015) Consumer reactions to intrusiveness of online-video advertisements: Do length, informativeness, and humor help (or hinder) marketing outcomes? *J. Advertising Res.* 55(1):37–50.
- Gorn GJ (1982) The effects of music in advertising on choice behavior: A classical conditioning approach. *J. Marketing* 46(1):94–101.
- Herget AK (2021) On music's potential to convey meaning in film: A systematic review of empirical evidence. *Psych. Music* 49(1):21–49.
- Hinton G, Deng L, Yu D, Dahl GE, Mohamed A-r, Jaitly N, Senior A, et al. (2012) Deep neural networks for acoustic modeling in speech recognition: The shared views of four research groups. *IEEE Signal Processing Magazine* 29(6):82–97.
- Holbrook MB, Batra R (1987) Assessing the role of emotions as mediators of consumer responses to advertising. *J. Consumer Res.* 14(3):404–420.
- Huang JT, Kaul R, Narayanan S (2022) Variety and risk-taking in content creation: Evidence from a field experiment using image recognition techniques. Preprint, submitted June 9, [https://papers.ssrn.com/sol3/papers.cfm?abstract\\_id=4126834](https://papers.ssrn.com/sol3/papers.cfm?abstract_id=4126834).
- Huron D (1989) Music in advertising: An analytic paradigm. *Music Quart.* 73(4):557–574.
- Jaquet L, Danuser B, Gomez P (2014) Music and felt emotions: How systematic pitch level variations affect the experience of pleasantness and arousal. *Psych. Music* 42(1):51–70.
- Johnson-Laird PN, Oatley K (2016) Emotions in music, literature, and film. Feldman Barrett L, Lewis M, Haviland-Jones JM, eds. *Handbook of Emotions*, 4th ed. (Guilford Press, New York), 82–97.
- Kallinen K, Ravaja N (2006) Emotion perceived and emotion felt: Same and different. *Music Sci.* 10(2):191–213.
- Kamins MA, Marks LJ, Skinner D (1991) Television commercial evaluation in the context of program induced mood: Congruency vs. consistency effects. *J. Advertising* 20(2):1–14.
- Kapoor A, Narayanan S, Sharma A (2022) Does emotional matching between video ads and content lead to better engagement: Evidence from a large-scale field experiment. Working paper, Stanford University, Palo Alto, CA.
- Kim YE, Schmidt EM, Migneco R, Morton BG, Richardson P, Scott J, Speck JA, Turnbull D (2010) Music emotion recognition: A state of the art review. *11th Internat. Soc. Music Inform. Retrieval Conf. (ISMIR 2010)*, vol. 86, 937–952.
- Krishna A (2012) An integrative review of sensory marketing: Engaging the senses to affect perception, judgment and behavior. *J. Consumer Psych.* 22(3):332–351.
- Krizhevsky A, Sutskever I, Hinton GE (2012) ImageNet classification with deep convolutional neural networks. *Adv. Neural Inform. Processing Systems* 25 (Lake Tahoe, NV), 1097–1105.
- Kutz JN, Brunton SL (2022) Parsimony as the ultimate regularizer for physics-informed machine learning. *Nonlinear Dynam.* 107(3):1801–1817.
- Lee CJ, Andrade EB, Palmer SE (2013) Interpersonal relationships and preferences for mood-congruity in aesthetic experiences. *J. Consumer Res.* 40(2):382–391.
- Li H, Lo HY (2015) Do you recognize its brand? The effectiveness of online in-stream video advertisements. *J. Advertising* 44(3): 208–218.
- Liu L, Dzyabura D, Mizik N (2020) Visual listening in: Extracting brand image portrayed on social media. *Marketing Sci.* 39(4): 669–686.
- Liu X, Chen Q, Wu X, Liu Y, Liu Y (2017) CNN based music emotion classification. Preprint, submitted April 19, <https://arxiv.org/pdf/1704.05665>.
- McAdams S, Giordano BL (2015) The perception of musical timbre. Hallam S, Cross I, Thaut M, eds. *The Oxford Handbook of Music Psychology*, 2nd ed. (Oxford University Press, Oxford, UK), 113–124.
- Melzner J, Raghubir P (2023) The sound of music: The effect of timbral sound quality in audio logos on brand personality perception. *J. Marketing Res.* 60(5):932–949.
- Müller M (2015) *Fundamentals of Music Processing: Audio, Analysis, Algorithms, Applications* (Springer, Cham, Switzerland).
- Nelson DJ, Grazier R, Paglia J, Perkowitz S (2013) *Hollywood Chemistry: When Science Met Entertainment* (American Chemical Society, Washington, DC).
- Panda R, Malheiros R, Paiva RP (2018) Novel audio features for music emotion recognition. *IEEE Trans. Affective Comput.* 11(4):614–626.
- Pavan MC, Dos Santos VG, Lan AG, Martins J, Santos WR, Deutsch C, Costa PB, Hsieh FC, Paraboni I (2023) Morality classification in natural language text. *IEEE Trans. Affective Comput.* 14(2):857–863.
- Pons J, Lidy T, Serra X (2016) Experimenting with musically motivated convolutional neural networks. *2016 14th Internat. Workshop Content-Based Multimedia Indexing (CBMI)* (IEEE), 1–6.
- Puccinelli NM, Wilcox K, Grewal D (2015) Consumers' response to commercials: When the energy level in the commercial conflicts with the media context. *J. Marketing* 79(2):1–18.
- Rajaram P, Manchanda P (2024) Unboxing engagement in YouTube influencer videos: An attention-based approach. Preprint, submitted August 6, <https://arxiv.org/pdf/2012.12311>.
- Ribeiro MT, Singh S, Guestrin C (2016) "Why should I trust you?" Explaining the predictions of any classifier. *Proc. 22nd ACM SIGKDD Internat. Conf.* (Association for Computing Machinery, New York), 1135–1144.
- Russell JA (1980) A circumplex model of affect. *J. Personality Soc. Psych.* 39(6):1161–1178.
- Selvaraju RR, Cogswell M, Das A, Vedantam R, Parikh D, Batra D (2020) Grad-CAM: Visual explanations from deep networks via gradient-based localization. *Internat. J. Comput. Vision* 128:336–359.
- Sisodia A, Burnap A, Kumar V (2024) Automatic discovery and generation of visual design characteristics: Application to visual conjoint. Preprint, submitted August 3, <http://dx.doi.org/10.2139/ssrn.4151019>.
- Stoppe S (2014) *Film in Concert. Film Scores and Their Relation to Classical Concert Music* (Verlag Werner Hülsbusch, Hamburg, Germany).

- Teeny JD, Siev JJ, Briñol P, Petty RE (2021) A review and conceptual framework for understanding personalized matching effects in persuasion. *J. Consumer Psych.* 31(2):382–414.
- Thompson WF, Balkwill LL (2010) Cross-cultural similarities and differences. Juslin PN, Sloboda JA, eds. *Handbook of Music and Emotion: Theory, Research, Applications* (Oxford University Press, Oxford, UK), 755–788.
- Toubia O, Berger J, Eliashberg J (2021) How quantifying the shape of stories predicts their success. *Proc. Natl. Acad. Sci. USA* 118(26):e2011695118.
- Troncoso I, Luo L (2023) Look the part? The role of profile pictures in online labor markets. *Marketing Sci.* 42(6):1080–1100.
- Unni D, D'Cunha AM, Deepa G (2022) A technique to detect music emotions based on machine learning classifiers. *2022 Second Internat. Conf. Interdisciplinary Cyber Physical Systems (ICPS)* (IEEE), 136–140.
- Wang X, He J, Curry DJ, Ryoo JH (2022) Attribute embedding: Learning hierarchical representations of product attributes from consumer reviews. *J. Marketing* 86(6):155–175.
- Wilbur KC (2008) A two-sided, empirical model of television advertising and viewing markets. *Marketing Sci.* 27(3): 356–378.
- Yang Y, Chen H (2011) Predicting the distribution of perceived emotions of a music signal for content retrieval. *IEEE Trans. Audio Speech Language Processing* 19(7):2184–2196.
- Yang J, Zhang J, Zhang Y (2023) First law of motion: Influencer video advertising on TikTok. Preprint, submitted August 18, <http://dx.doi.org/10.2139/ssrn.3815124>.
- Yang J, Xie Y, Krishnamurthi L, Papaita P (2022) High-energy ad content: A large-scale investigation of TV commercials. *J. Marketing Res.* 59(4):840–859.
- Zhang M, Luo L (2023) Can consumer-posted photos serve as a leading indicator of restaurant survival? Evidence from Yelp. *Management Sci.* 69(1):25–50.